ADVANCED SENSOR RESEARCH Open Access
www.advsensorres.com

Aggregation-Induced Emission Luminogens for Gas Sensors

*Yongbo Yu, Si-Wei Zhang, Jinhui Jiang, Fulong Ma, Richard Wang, Tonghui Huang, Jianwei Zhao, Chao He, and Guodan Wei**

Luminescent chromophores armed with aggregation-induced emission (AIE) characteristics can switch their fluorescence sensing by manipulating the aggregation and disaggregation states, leading to high sensitivity and high signal-to-noise ratio sensors. Accordingly, aggregation-induced emission luminogens (AIEgens) have been widely applied to various biosensing, one of which is the gas sensors. Due to the weak signal, easy diffusion, difficult capture, and instability of gas molecules, electrochemical or infrared tests are generally used for detection. However, electrochemical tests have high power consumption, and the environment easily disturbs infrared tests. Fortunately, photochemical sensors utilizing AIE properties can effectively overcome these deficiencies. AIEgens usually exhibit large Stokes shift, good photostability, and low random blinking, suggesting excellent sensing reproducibility and many achievements have been obtained in AIEgens-based gas sensors. This review summarizes the gas detection mechanism of AIEgens, and enumerate the reported gas sensors based on AIEgens. Then a perspective on the field and challenges facing it are elaborated so that researchers can better understand the development status of this field and develop more AIE-type spectroscopic probes with gas-responsive functions. It is expected to greatly enrich the types of gas sensors and promote the development of the application of AIE properties.

1. Introduction

Fluorescence sensing, one of the most widely used biochemical and chemical analytes, has been successfully applied to clinical, bioprocess, and environmental fields.[1–4] The technology not only provides rapid real-time detection of different types of analytes but also qualitatively and quantitatively them by their distinct fluorescence changes.[5–7] However, the fluorescent molecules utilized by the early-developed fluorescent sensors mainly belong to solution-state luminescent molecules such as rhodamine,[8,9] coumarin,[10,11] etc. These molecules exhibit strong fluorescence in solution, but when their concentration increases or aggregates, the fluorescence intensity decreases or quenches. This phenomenon is called aggregation-induced luminescence quenching (aggregation-caused quenching, ACQ).[12] The ACQ effect is not favorable to the development of fluorescent sensors, so researchers have adopted various strategies to avoid it, but the impact of their attempts has been limited. This was until 2001 when Ben Zhong Tang's group proposed an aggregation-induced luminescence (AIE) concept based on the phenomenon that a propeller-shaped molecule (hexaphenylsilole) emits weak or no light in the solution state but strongly emits light in its aggregated or solid-state (**Figure 1**).[13] The proposal of this AIE concept provides a new strategy for the development of fluorescent sensors.

After two decades of development, several mechanisms have been put forward to explain the interesting AIE phenomenon

Y. Yu, S.-W. Zhang, G. Wei
Tsinghua-Berkeley Shenzhen Institute
Institute of Materials Science
Tsinghua Shenzhen International Graduate School
Tsinghua University
Shenzhen 518055, China
E-mail: weiguodan@sz.tsinghua.edu.cn

The ORCID identification number(s) for the author(s) of this article can be found under https://doi.org/10.1002/adsr.202300027

DOI: 10.1002/adsr.202300027

Y. Yu, T. Huang
School of Pharmacy
Xuzhou Medical University
Xuzhou 221004, China

J. Jiang, F. Ma
School of Science and Engineering
Shenzhen Institute of Aggregate Science and Technology
The Chinese University of Hong Kong
Shenzhen 518172, China

R. Wang
Mountain View High School
Mountain View, CA 94040, USA

J. Zhao
Shenzhen HUASUAN Technology Co. Ltd.
Shenzhen 518055, China

C. He
Department of Engineering Science
University of Oxford
Parks Road, Oxford OX1 3PJ, UK

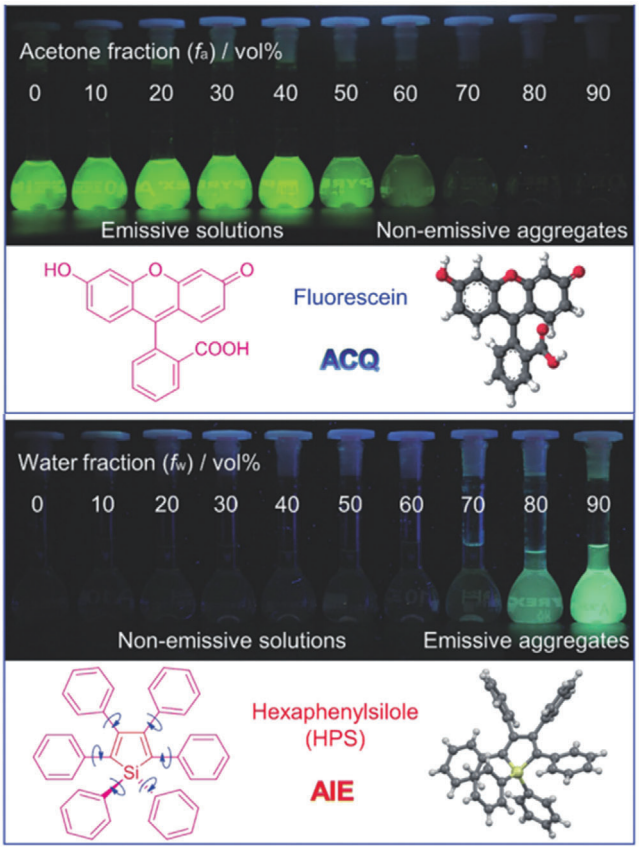

Figure 1. Photos of the ACQ effect of fluorescein and AIE activity of HPS in the mixture of miscible water and organic solvent. Reproduced with permission.[13] Copyright 2001, Royal Society of Chemistry.

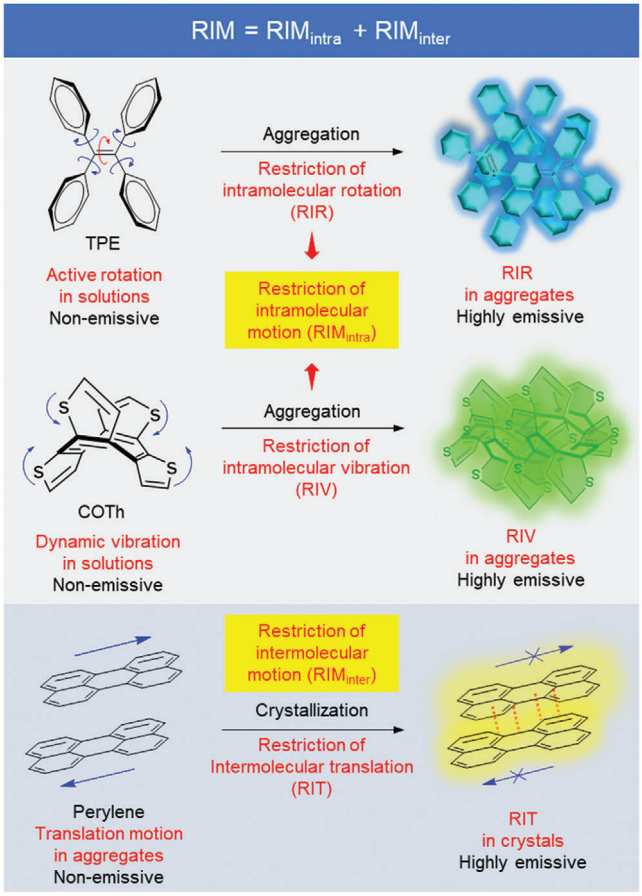

Figure 2. Typical examples of AIEgens and the primary mechanism for their AIE processes. The AIE processes of TPE, COTh, and perylene ascribe to RIR, RIV, and RIT, respectively. Reproduced with permission.[16] Copyright 2022, Wiley-VCH.

based on many experiments and theoretical verifications.[14–16] **Figure 2** lists the typical aggregation-induced emission luminogens (AIEgens) and the primary mechanism for their AIE processes. Tetraphenylethene (TPE), the most thoroughly studied AIEgen, almost has no fluorescence in the solution state due to the energy dissipation by active molecular rotation (Rotation of the benzene ring and twist of the C=C bond) in its excited state. However, it is highly luminescent when forming aggregates. TPE's AIE process is mainly ascribed to the restriction of intramolecular rotation (RIR).[17] Cyclooctatetrathiophene (COTh), a rotor-free AIEgen, also exhibits a similar AIE phenomenon to TPE. Both the experimental and theoretical results certify that excited-state intramolecular vibrations lead to weak emission of COTh in the solution. The bright green emissions from the aggregated state originate from the restriction of intramolecular vibration (RIV).[18] However, in some cases, the molecules' loosely packed aggregation shows scarcity emission as the molecular motions can still enhance the nonradiative transitions. Perylene shows dim emission in amorphous powder but bright yellow emission in the ordered crystal due to the restriction of intermolecular motion (RIT).[15,16] When AIEgens are molecularly dispersed and isolated, the molecular motions dominate the dissipation of excitation energy and the restriction of the molecular motions is in favor of the radiative decay.

Accordingly, fluorescence sensing switches can be manipulated by controlling the aggregation and disaggregation of AIEgens, leading to low background and high signal-to-noise ratio sensors. Furthermore, AIEgens usually exhibit good photostability, strong photobleaching resistance, large Stokes shift, and low random blinking, suggesting excellent sensing reproducibility.[19–22] Based on these wonderful properties, many achievements have been obtained by applicating the AIEgens in various biosensing. And several approaches, including regulation of electrostatic interaction and hydrogen bond interaction, cleavage by chemical moieties or enzymes, charge transfer or electron transfer, aggregation-enhanced emission (AEE), encapsulation or nanoprecipitation, and target-induced disaggregation or quenching, were proposed to manipulate the molecule behavior (**Figure 3**).[23–26] These methods motivate more extensive development of the AIEgens on biosensing.

Among the many fluorescence sensing applications of AIEgens, the gas sensor is an important category.[27–29]

There are three main methods of gas detection: the non-dispersive infrared method, the semiconductor method, and the electrochemical method. Non-dispersive infrared method gas sensor utilizes the property that gas molecules absorb infrared

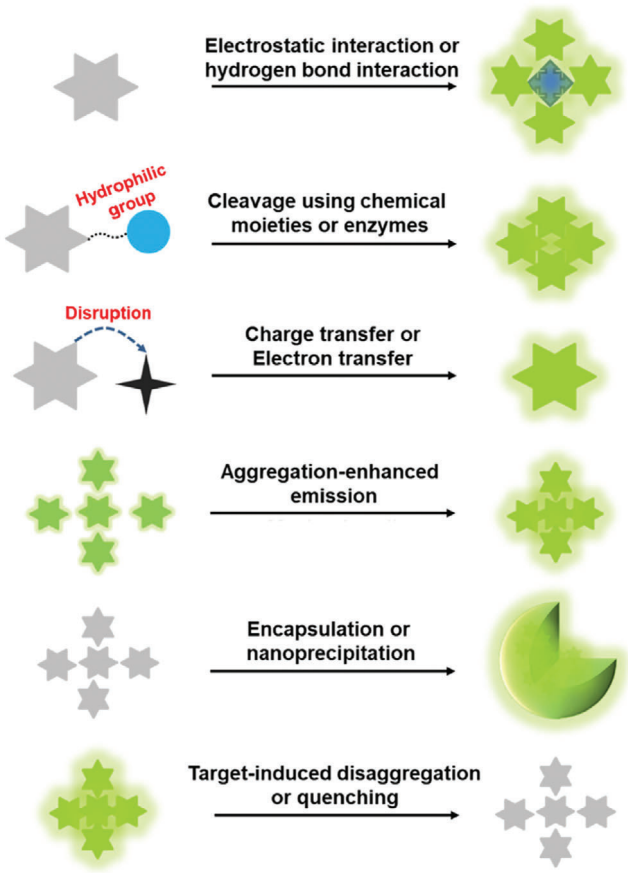

Figure 3. Schematic diagram of the methods for regulating AIEgens for fluorescence sensing. Reproduced with permission.[23] Copyright 2020, Wiley-VCH.

rays at specific wavelengths, which consists of a light emitter, an infrared sensor, and an optical cavity. The infrared rays emitted by the infrared light or source gas molecules in the optical cavity reach the infrared sensor after being attenuated. The gas concentration can be calculated based on the difference in the amounts of infrared radiations reached. The semiconductor gas sensor calculates the gas concentration by using the change of resistance value after the reaction between the heated metal oxide and gas. Electrochemical gas sensors use oxidation-reduction reactions to measure gas concentration. The gas molecules to be detected undergo an oxidative reaction at a sensing electrode, generating ions and electrons. Ions are transferred to the counter electrode via an electrolyte and electrons are transferred to a counter electrode via an external circuit, resulting in a reduction.[30] Due to their weak signal, easy diffusion, difficult capture, and instability of gas molecules, electrochemical tests or infrared tests are generally used for detection. However, electrochemical tests have high power consumption, and infrared tests are easily disturbed by the environment.[30–32] Fortunately, photochemical sensors utilizing AIE properties can effectively overcome these deficiencies.[33,34] Although many AIEgens for gas detection have been reported, quantities are still limited in general. This review will summarize the gas detection mechanism of AIEgens, and enumerate the reported gas sensors based on AIEgens. Eventually, we will elaborate on the perspective and challenges in this emerging field so that researchers can better understand the development status of this field and develop more AIE-type spectroscopic probes with gas-responsive functions. It will greatly enrich the types of gas sensors and promote the development of the application of AIE properties.

2. The Mechanism of AIEgens for Gas Sensor

The gas detection mechanism of AIEgens can be divided into two categories: reactive and non-reactive. Reactive AIEgens probe refers to the chemical reaction between AIE molecules and their target, resulting in the change of molecular structure. Reactive AIEgens probes generally have better selectivity and sensitivity.[35] Reactive AIEgens probes are a unique method for detecting gaseous targets.

Non-reactive AIEgens fluorescent probes are mainly based on the interaction forces between AIEgens and targets, such as van der Waals forces between host and guest, hydrogen bonds, etc. Non-reactive probes are generally reversible and can be reused multiple times. Hydrogen bonding is an intermolecular force weaker than ionic and covalent bonds but stronger than van der Waals forces.[36] The formation of intramolecular hydrogen bonds in AIEgens restricts intramolecular motion and generates excited state intramolecular proton transfer (ESIPT). The construction of aggregates caused by the AIE effect favors the onset of the ESIPT process, and if the process of proton transfer from the donor to the acceptor in the excited state is hindered, the fluorescence emission spectrum will shift.[37] Electrostatic interaction is a force that holds two oppositely charged substances together. The hydrophobic interaction mainly utilizes the principle that non-polar molecules quickly form aggregates in an aqueous solution.[38]

3. The Development of AIEgens for Gas Sensor

Dong et al. firstly analyzed the influence of solvent vapor on the luminescence property of the 2,3,4,5-tetraphenylsiloles with different 1,1-substituents (molecules **1–4**).[39] These silole spots on the TLC plates show tunable luminescence and the ability to turn them on and off by the fumigation and volatilization of organic solvent vapors (**Figure 4**). By immersing the TLC plate in a solvent atmosphere several times and drying it, surprisingly, this process is reversible, suggesting the compound can be used as a detector for organic solvents. The tunable emission ascribes the morphology transformation from the amorphous by fumigation to the crystalline phase by evaporating the solvent.

Following the pioneering work, AIEgens-based probes have detected various gases, including carbon dioxide, formaldehyde, methanol, hydrochloric acid, amines, hydrogen sulfide, and more. **Scheme 1** lists the structure of the molecules or AIEgens employed as the gas sensors.

3.1. Carbon Dioxide (CO_2)

CO_2 is the primary greenhouse gas leading to global warming, and its impact on the environment has attracted widespread

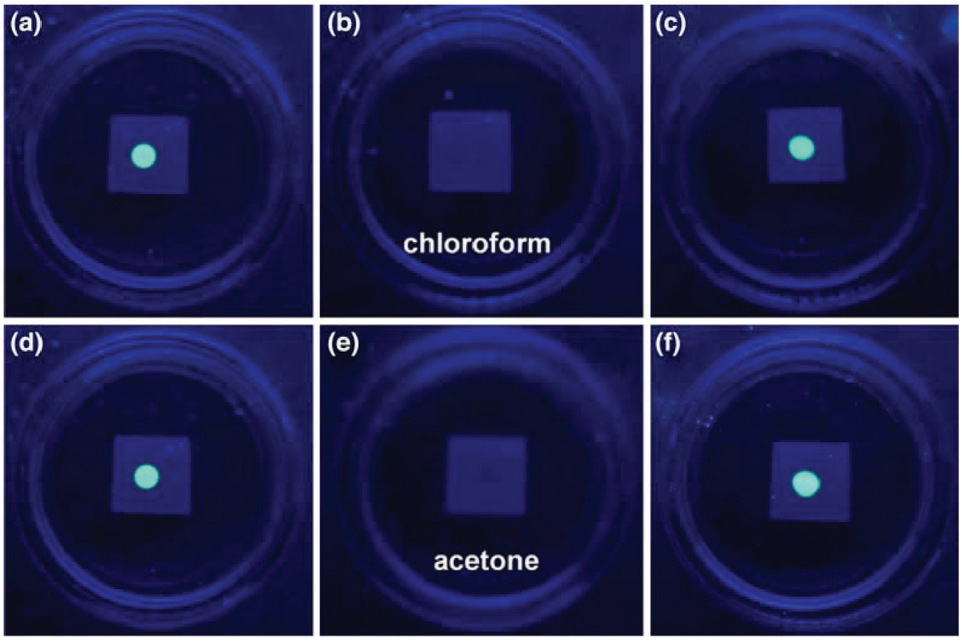

Figure 4. a,d) Original spots of molecule **2** on the TLC plates. b,e) Exposure to the spots to chloroform and acetone vapors for about 1 min. c,f) Taken in about 2 min after the solvents were evaporated. All the photographs were taken under UV illumination at room temperature. Reproduced with permission.[39] Copyright 2007, Springer.

attention.[40] Additionally, CO_2 is a significant health and safety concern for workers working in confined spaces. Long-term exposure to high concentrations (above 3000 ppm) of CO_2 can cause health problems (the average concentration of CO_2 in the atmosphere is about 400 ppm), resulting in some physiological dysfunction and irreversible damage to organs.[41] The current commercial CO_2 sensors are mainly based on infrared spectral detectors, which have poor sensitivity and high costs.[42] Therefore, it is necessary to develop fast and convenient CO_2 sensors.

Ma et al. have created two fluorescent CO_2 gas sensors based on the xerogel films and gel aggregates of AIEgens **5**.[43] Compound **5** is a good gelator in many aromatic solvents, and it can form a host-guest complex with carbamate ionic liquid counter anion. Devices used for gas detection need to have a larger specific surface area to enhance the detection capability. Since the gel state is not conducive to preparing gas sensors, a gel into xerogel film was designed. The xerogel films can be easily fabricated from gels, showing high specific surface area and porosity with good stability. As shown in **Figure 5**, the xerogel films of **5** had a sky-blue emission of 460 nm. When exposed to CO_2 gas, the fluorescence intensity of xerogel film decreases, and the fluorescence intensity decay shows an excellent linear relationship with CO_2 concentration in the range of 0–2000 ppm. With the further increase of CO_2 concentration, the fluorescence intensity of xerogel film decreased, and a new emission peak appeared around 550 nm. The films achieved a sensitivity and low detection limit of 4.5 ppm. The naked eye can detect the CO_2 response on the xerogel films, making the system promising for constructing xerogel-based devices for CO_2 detection for practical applications.

Xie et al. created a prototype CO_2 fluorescence sensor based on a real dynamic AIE-active metal–organic frameworks (MOFs) (anthracene 9,10-diacrylate acid (ADA)–Mn), as shown in **Figure 6a**.[44] MOFs usually have large specific surface areas and excellent mechanical properties, making them a perfect support material. **6** shows the ACQ effect due to the anthracene with green emission. While after self-assembly with ADA (**6**) and Mn(II), an AIE-type MOF was gained. The fluorescence intensity shows a linear relationship with the viscosity of DMF/glycerol mixed solution. The AIE process origins from the J-aggregate of **6** during the nanoparticle collision, so the fluorescence intensity also changed with the particle size. The unanticipated transition from ACQ to AIE provides a new design strategy for novel AIE-type MOFs structures. When bubbled the CO_2 gas into dipropylamine, the fluorescence intensity (I) keeps increasing, and the $\log_{10} I$ versus CO_2 volume shows a good linear relationship, suggesting the potential of ADA–Mn MOFs for CO_2 gas sensors.

3.2. Formaldehyde (HCHO)

Formaldehyde is a common carcinogenic toxic aldehyde, which can react with nucleophilic material and lead to irreversible damage to DNA.[45] Smalldoses of formaldehyde results in emesis, pain, and stupor, and large amounts of formaldehyde can cause death.[46] Formaldehyde was categorized in Group I as carcinogenic to humans in 2004, and the WHO suggested the limit of formaldehyde as 0.15 mg kg^{-1}.[47] However, formaldehyde is very common in life. It may be artificially added to frozen food storage, processing, paint, furniture, and other items, therefore making it easy to become exposed to this dangerous gas. Hence, it is critical to developing fluorescent sensors for formaldehyde detection.

Bi et al. designed a formaldehyde fluorescent probe **7** with a 1,8-Naphthalimides core.[48] 1,8-Naphthalimides bears strong

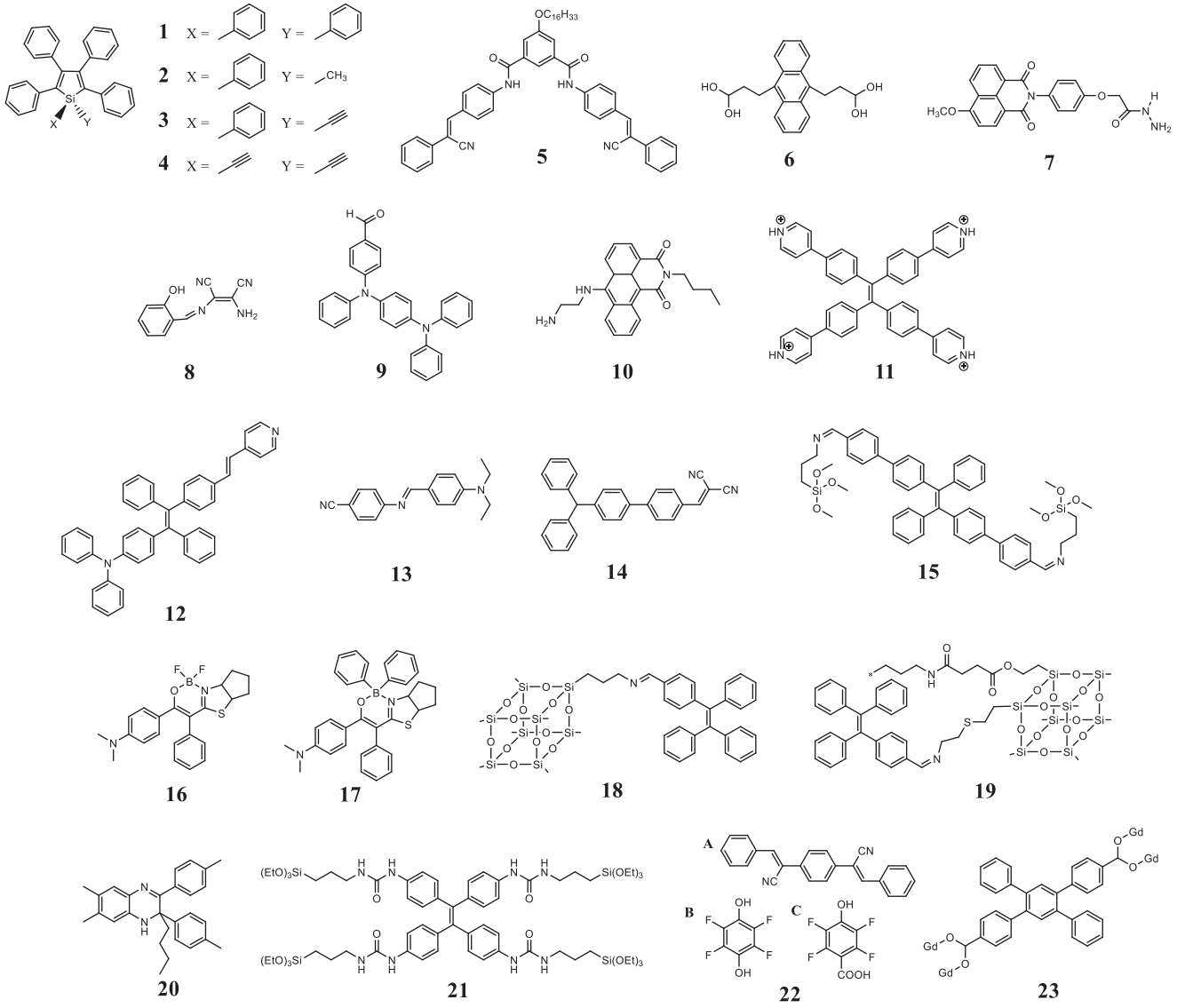

Scheme 1. The molecular structure of AIEgens for gas sensors.

electron donation, making the optical properties to be easily transformed by intramolecular charge transfer (ICT) and photo-induced electron transfer (PET).[49] As shown in **Figure 7**a, the PET process of molecular **7** could be suppressed by the addition of formaldehyde, leading to a visible increase in fluorescence intensity and a color change. Probe **7** shows weak blue emission (440 nm) in DMF/H_2O mixed solution, and the emission peak red-shift to 525 nm with a dramatically enhanced fluorescent intensity with the addition of the formaldehyde. The ^{1}H NMR titration experiment shows how the amino protons' signal of hydrazine decreases and protons of Schiff base increase after the reaction, indicating the hydrazine unit has generated Schiff base form. The detection limit of probe **7** for formaldehyde was determined to be 20 nM based on the signal-to-noise ratio, suggesting that **7** can detect formaldehyde with high sensitivity. Furthermore, the probe could detect formaldehyde rapidly (6 min) in an aqueous solution.

Lin et al. created a prototype formaldehyde probe **DP5J** based on bis-thioacetylhydrazine-functionalized pillar[5]arene (**Figure 8**a).[50] The hydrazide groups on **DP5J** function as the formaldehyde reaction recognition and hydrogen bonding self-assembly sites, and the pillar[5]varene group acts as the $\pi...\pi$ stacking site to facilitate the AIE property. With the preplaced catalyst ($(CF_3SO_3)_2Bi$), **DP5J** exhibits ultrasensitive formaldehyde ability with a response time of 7.5 s and a detection limit of 3.27 nM. Furthermore, DP5J also shows recognized formaldehyde selectively among the many aldehydes (Figure 8b) and naked eyes can distinguish the emission color change. The Tyndall effect confirms the aggregation process in **DP5J** + formaldehyde + catalysts $(CF_3SO_3)_2Bi$ system. As shown in Figure 8c, before adding formaldehyde, the **DP5J** + catalysts $(CF_3SO_3)_2Bi$ solution shows no Tyndall phenomenon; however, an apparent Tyndall phenomenon shows up immediately when adding the formaldehyde to the solution, suggesting the aggregation of colloid particles

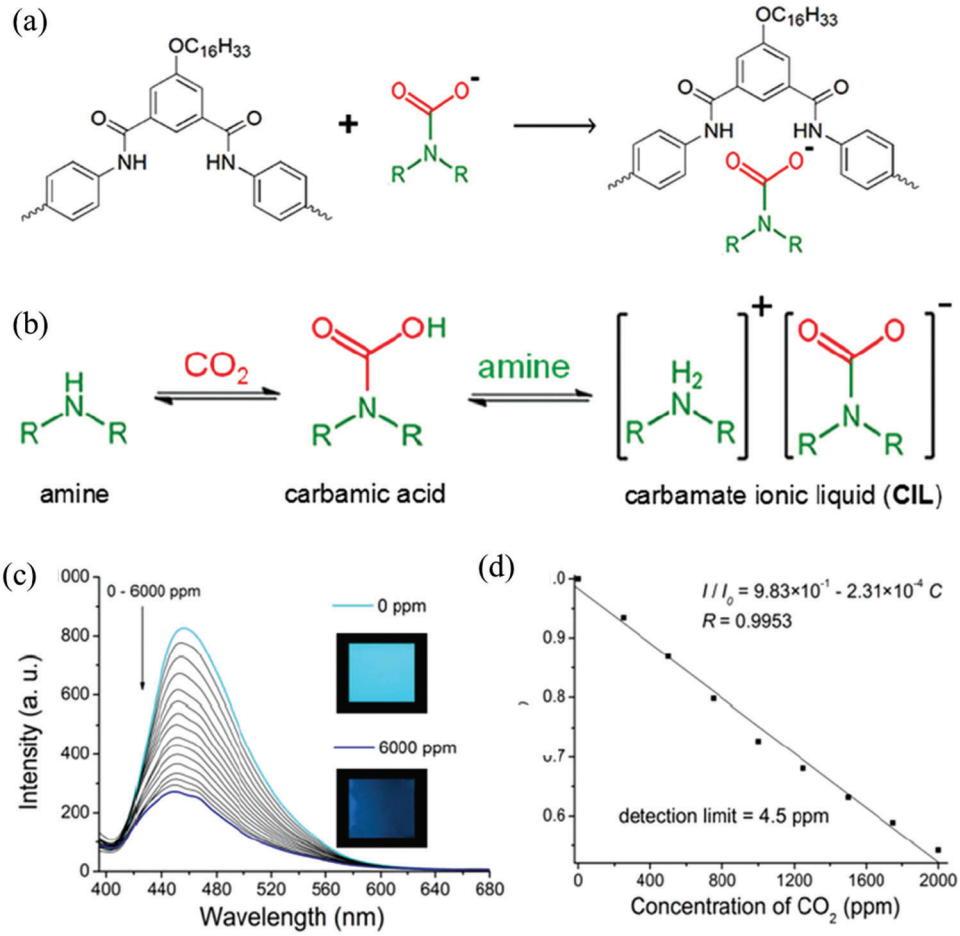

Figure 5. a) The proposed mechanism between **5** and the carbamate ionic liquid counter anion formation host–guest complex. b) Reaction scheme of forming a CIL by CO_2 and an aliphatic amine. c) Emission spectra of the xerogel film exposed to different concentrations of CO_2 with aliphatic diethylamine (DEA) vapor and d) plot of the fluorescence intensity change versus different concentrations of CO_2. Reproduced with permission.[43] Copyright 2018, Royal Society of Chemistry.

formed, agree with the supposed formaldehyde recognition mechanism in Figure 8a. A silica gel plate loaded with **DP5J** + catalysts $(CF_3SO_3)_2Bi$ was prepared to facilitate formaldehyde detection. The fluorescence was turned on when dipping into different concentrations of formaldehyde solution (from 1 M to 1 nM) as well as placed in formaldehyde vapor. Distinct fluorescence emission changes with the amount of formaldehyde, indicating the silica gel plates could function as an efficient and ultrasensitivity formaldehyde sensor for both formaldehyde vapor and solution.

Fan's group reported several AIEgens-based fluorescence sensors with good sensitivity and practical values from Schiff base derivatives.[51–54] As shown in **Figure 9**a, probe **8** with the binding sites of C = N,–NH_2 can monitor formaldehyde and hypochlorites with visible color change by the naked eye. The fluorescence emission keeps decreasing as the increasing of formaldehyde concentration and shows an excellent linear relationship between the fluorescence intensity and formaldehyde concentrations, implying that probe **8** could y detect aqueous formaldehyde quantitatively. And the detection limit is calculated as 42 nM, suggesting the high sensitivity of the probe. The good fluorescence-sensing ability of probe **8** can be attributed to the intramolecular charge transfer between the electron push/pull system. When **8** was exposed to the amino group binds with formaldehyde, the push–pull electron system is destroyed, so the fluorescence from **8** is quenched. Benefiting from the excellent solid-state luminescence properties of AIEgens, the fluorescent test paper prepared from probe **8** can achieve efficient and sensitive detection of gaseous formaldehyde.

3.3. Chlorine (Cl_2)

Chlorine is a highly toxic gas that can attack the human respiratory system, eyes, and skin.[55,56] What's worse, Cl_2 can react with water in the lungs, producing hydrochloric acid (HCl) and hypochlorous acid (HClO). Chlorine tends to gather at the bottom of poorly ventilated spaces because it is denser than air. When chlorine concentration exceeds 30 ppm, it can lead to coughing, vomiting, and even lung damage at 60 ppm. When the concentration is above 1000 ppm, it can be fatal after a few deep breaths.[57,58] Chlorine was destructive to living tissue and very

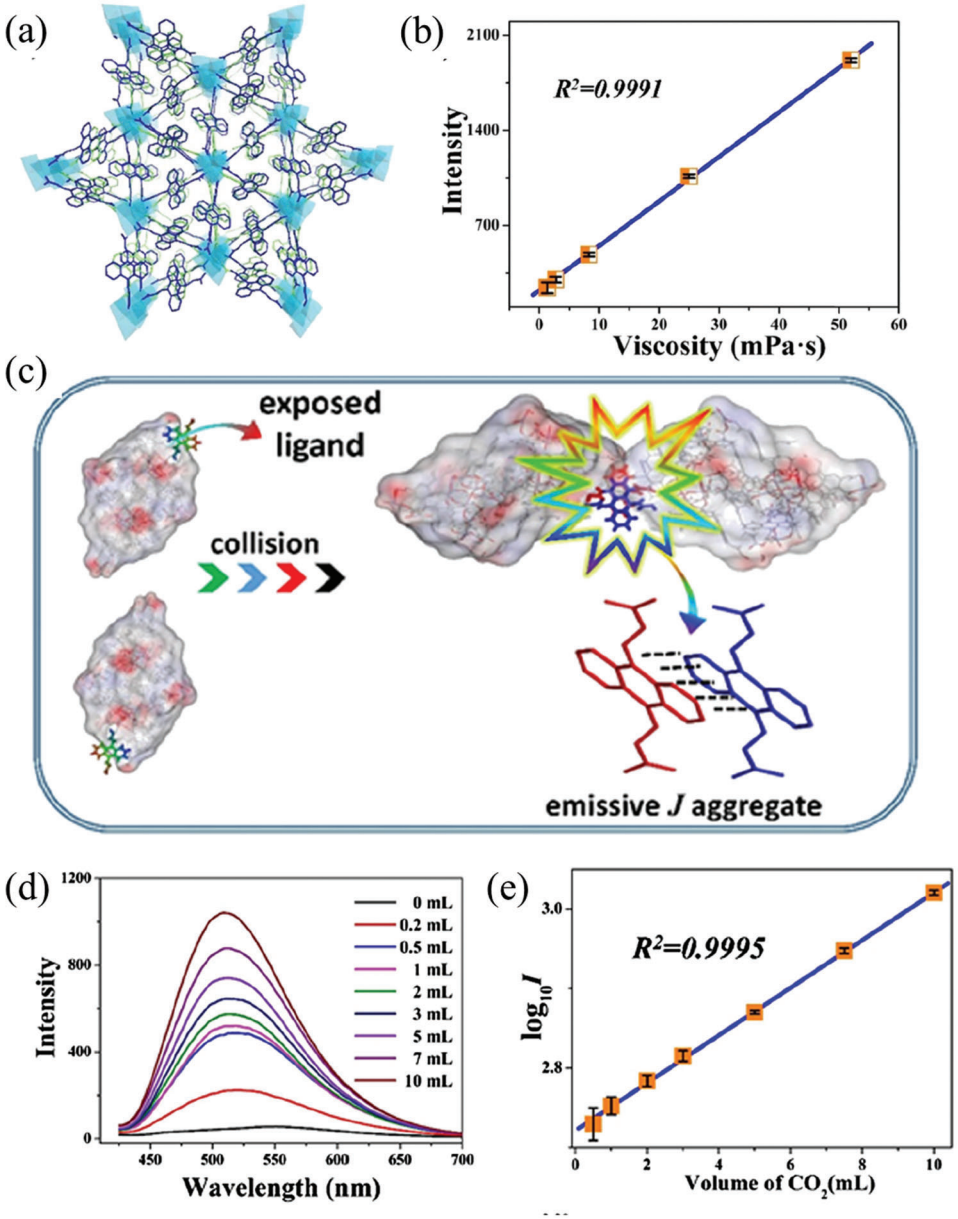

Figure 6. a) The three-dimensional conformation of ADA–Mn. b) fluorescence intensity versus the viscosity of DMF/glycerol mixed solution. c) Schematic diagram of the J-aggregate formation with collision-dictated. d) Fluorescence spectra of ADA–Mn dispersed in dipropylamine upon bubbling with different amounts of CO_2 gas. And e) the relationship between fluorescence intensity versus CO_2 volume. Reproduced with permission.[44] Copyright 2018, ACS.

lethal. Chlorine is also a strong oxidizer, which may be a potential fire threat when reacting with flammable materials. Given the huge harm of chlorine to the human body, developing a highly efficient and sensitive chlorine sensor is of great practical value.[59,60]

Ning et al. designed and synthesized **9** with diphenylamine as the electron donor and aldehyde as the electron acceptor, which shows good emission in the solid-state.[61] The AIE feature overcomes the problem of solid-state quenching fluorescence so that probe **9** still has bright luminescence in the thin film state. When the film of **9** was exposed to Cl_2, its fluorescence was immediately quenched (**Figure 10**b), and its absorption spectrum also showed significant intensity decay and the absence of the 360 nm peak. Previous research has found that triphenylamine could react with Cl_2 and obtain tris-pentachlorophenylamine in the solid state.[62,63] And the mass spectrum of probe **9** after being treated by Cl_2 also shows about ten groups of new signals, with the gap of each being about 35, suggesting several products with different numbers of chlorine atoms. Solid-state materials with strong fluorescence are desirable in a sensing system for high sensitivity to trace quantities, and AIE-active probes show great advantages in this field.

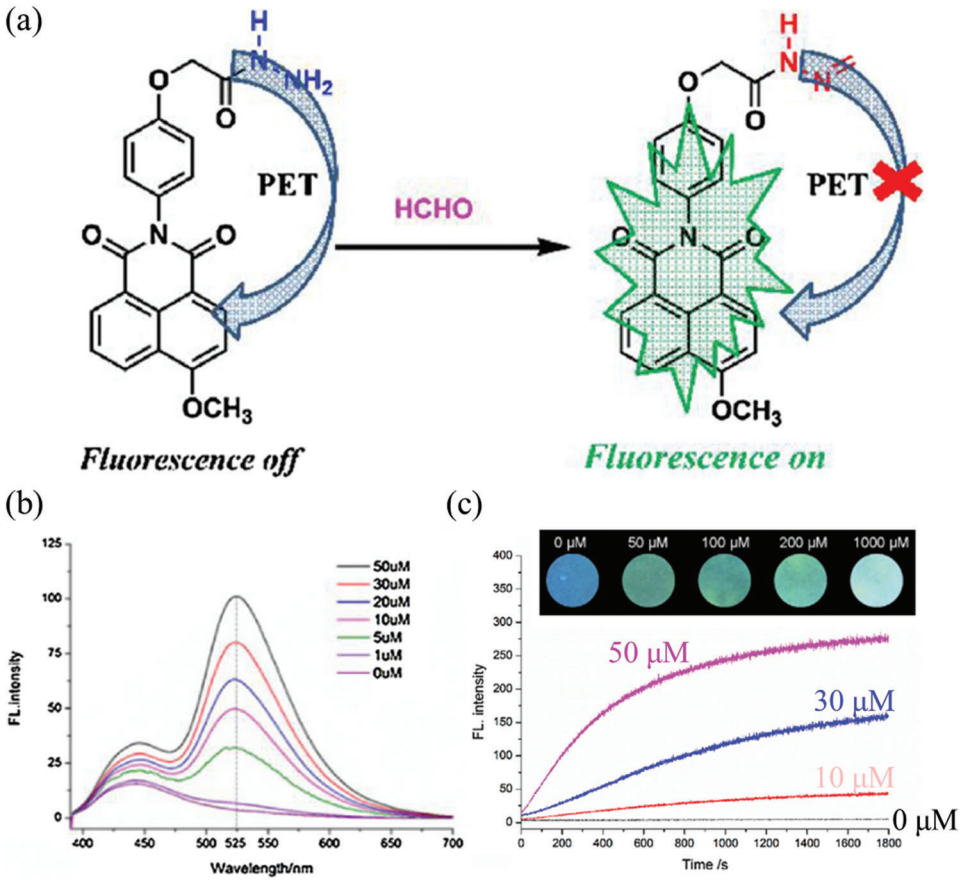

Figure 7. a) The photo-induced electron transfer (PET) mechanism of **7** detection formaldehyde. b) Fluorescence spectra of **7** in a mixed solution of DMF/H_2O upon adding different formaldehyde volumes. And c) Time-dependent PL intensity changes of **7** at 525 nm in different formaldehyde volumes (0, 10, 30, 50 μM). Inset: Photos of probe **7** (10 μM) for detecting formaldehyde at various concentrations. Reproduced with permission.[48] Copyright 2018, Elsevier.

3.4. Phosgene ($COCl_2$)

Phosgene is highly toxic, colorless, and odorless and was used as a chemical weapon.[64–66] The high toxicity of phosgene results from the action on the –OH, $–NH_2$, and –SH groups of proteins in the alveoli, which form esters, amides and thioesters, respectively. Phosgene disrupts the blood-air barrier, eventually leading to pulmonary edema. People affected by phosgene may experience no symptoms for several hours until pulmonary edema becomes irreversible.[67] Many chemists who use phosgene experience chronic respiratory health problems and eventually respiratory failure from exposure to phosgene at low and sustained levels. In industry, the mixture of carbon monoxide and chlorine can produce phosgene under light.[68] In UV light and oxygen presence, simple organochlorine compounds such as chloroform slowly become phosgene. Considering the huge hazards and difficult identification of phosgene, developing highly sensitive fluorescent indicators of nitrous oxide is crucial for related industries and chemists.

Liu et al. reported a fluorescent probe **10**, with an anthracene carboximide as thefluorophore and ethylenediamine group as the recognition moiety for phosgene detection.[28] Probe **10** shows good sensing ability for both solution and gaseous phosgene. As shown in **Figure 11**a, after exposure to the TLC plate loaded with **10** in phosgene vapor for 1 min, the red emission turns to yellow, and the yellow color gets deeper when increasing the phosgene amount. This change is more evident in the spectrogram, and the fluorescence intensity ratio (I_{520}/I_{610}) shows an excellent linear relationship with the amount of phosgene. Among the various analytes, **10** shows specificity for the detection of phosgene. The portable and reliable TLC plate for sensing gaseous phosgene based on probe **10** provides a valuable method to monitor phosgene leaks at phosgene-related facilities in practice. The ^{1}H NMR spectrum of **10** before and after exposure to phosgene confirmed that the mechanism for detecting phosgene was intramolecular charge transfer. The colorimetric and ratiometric probe **10** could respond to phosgene in a high sensibility way with a response time of fewer than 20 s and the limit of detection is 0.09 nM.

3.5. Nerve Agent

Nerve agents are some of the biggest threats to global security. Its manufacturing cost is low, and its preparation method is simple. Terrorists can use nerve agents to attack military and civilian targets.[69] Chemically, nerve agents, for example, tabun, so-

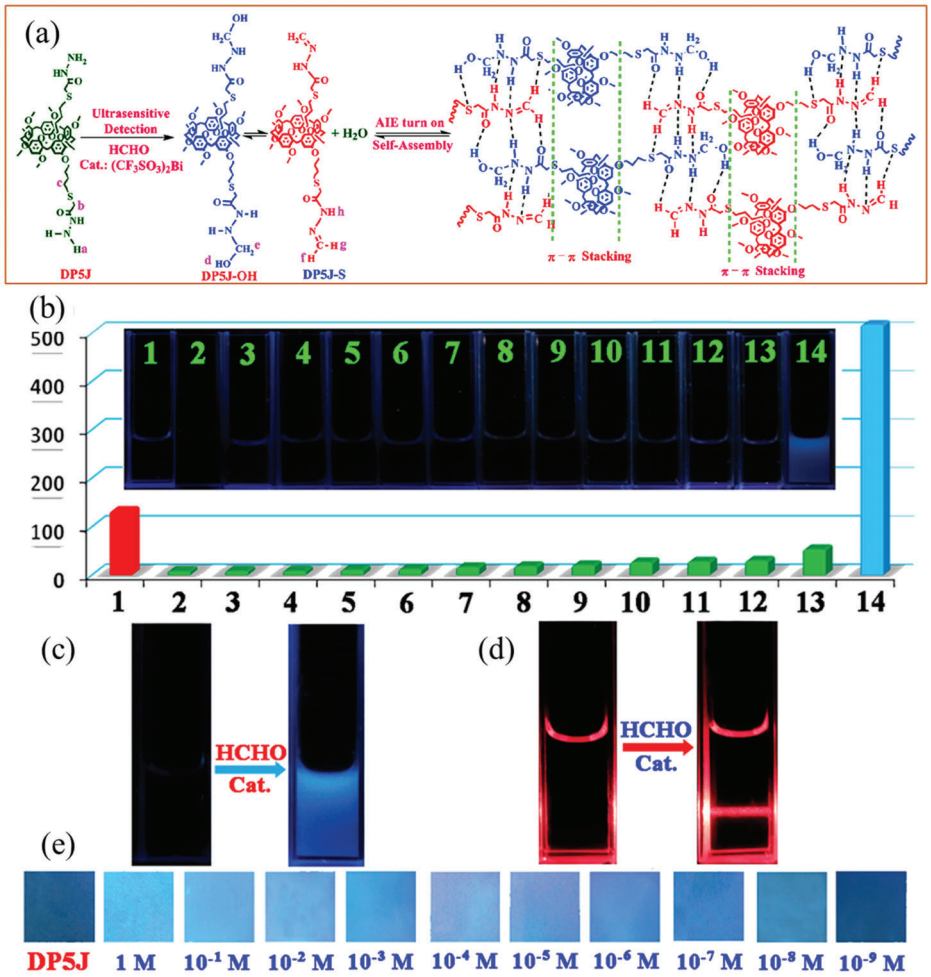

Figure 8. a) Proposed mechanism of **DP5J** for the detection of formaldehyde. b) Photos and fluorescence intensity of **DP5J** in different aldehydes. (1. DP5J only; 2. benzaldehyde; 3. salicylaldehyde; 4. p-fluorobenzaldehyde; 5. m-bromo-benzaldehyde; 6. p-chlorobenzaldehyde; 7. p-bromobenzaldehyde; 8. n-caprylaldehyde; 9. p-tolualdehyde; 10. m-chlorobenzaldehyde; 11. o-bromobenzaldehyde; 12. m-fluoro-benzaldehyde; 13. glutaraldehyde; 14. formaldehyde). c) Photos of **DP5J** and **DP5J** + formaldehyde + catalysts $(CF_3SO_3)_2Bi$ in DMF. d) Tyndall effect of the **DP5J** and **DP5J** + formaldehyde + catalysts $(CF_3SO_3)_2Bi$ in DMF. d) Photos of silica gel plate treated by **DP5J** + catalysts $(CF_3SO_3)_2Bi$ + different concentrations of formaldehyde (from 0 to 10^{-9} M). Reproduced with permission.[50] Copyright 2018, ACS.

man, and sarin are highly toxic organophosphates, paralyzing the central nervous system, resulting in organ decay and even death.[70,71] Even more frightening is that these nerve agents are colorless, odorless, and highly volatile. Because of the high toxicity and unavailability of nerve agents, a similar chemical compound, diethyl chlorophosphate (DCP), is typically used as a nerve gas-mimic for scientific study.[72,73]

Huang et al. fabricated a handy pen for sensing the DCP based on AIE-probe **11** (**Figure 12**a).[27] The pen-like portable sensor based on solid-phase microextraction is simple, miniaturized, and can rapidly detect gaseous compounds. When the fibers loaded with **11** are exposed to DCP vapor, the electrophilic pyridine group on **11** is attacked by the phosphonyl group on DCP, and the fluorescence emission color change from yellow to blue, which is visible by the naked eye. The color change is closely related to the DCP concentration and exposure time. As shown in Figure 12b, for the low DCP concentration, like 0.01 ppm, the color change in 60 min, while as the DCP concentration increases, the color change time decreases. The fiber emission can change in 30 min at a high concentration of 0.3 ppm. The calculated limit of detection for DCP is 3.4 ppb, suggesting the high sensitivity of the AIE handy pen sensor. This portable device can be ported to other AIE probes to detect various gas analytes. For example, probe **20** can be assembled on the fiber to monitor NH_3 (Figure 12c), achieving a fast and sensitive amine sensor.

Huang et al. designed a portable sensor for ratiometric fluorescence based on AIE probe **12** to sensor DCP vapor by a paper strip.[74] With typical AIE properties, probe **12** shows strong emission in the solid state. The pyridine group of **12** has strong nucleophilicity and will be first electrophilically reacted with the phosphonyl group at DCP. Subsequently, the N—P bond reacts with a weak nucleophilic reagent, such as oxygen atoms from water and is hydrolyzed into pyridinium salt. The initial yellow fluorescence emission peak at 546 nm changes to orange-red emission around 624 nm. And the peak intensity of 624 nm keeps increasing with the DCP concentration goes high, as shown in **Figure 13**c.

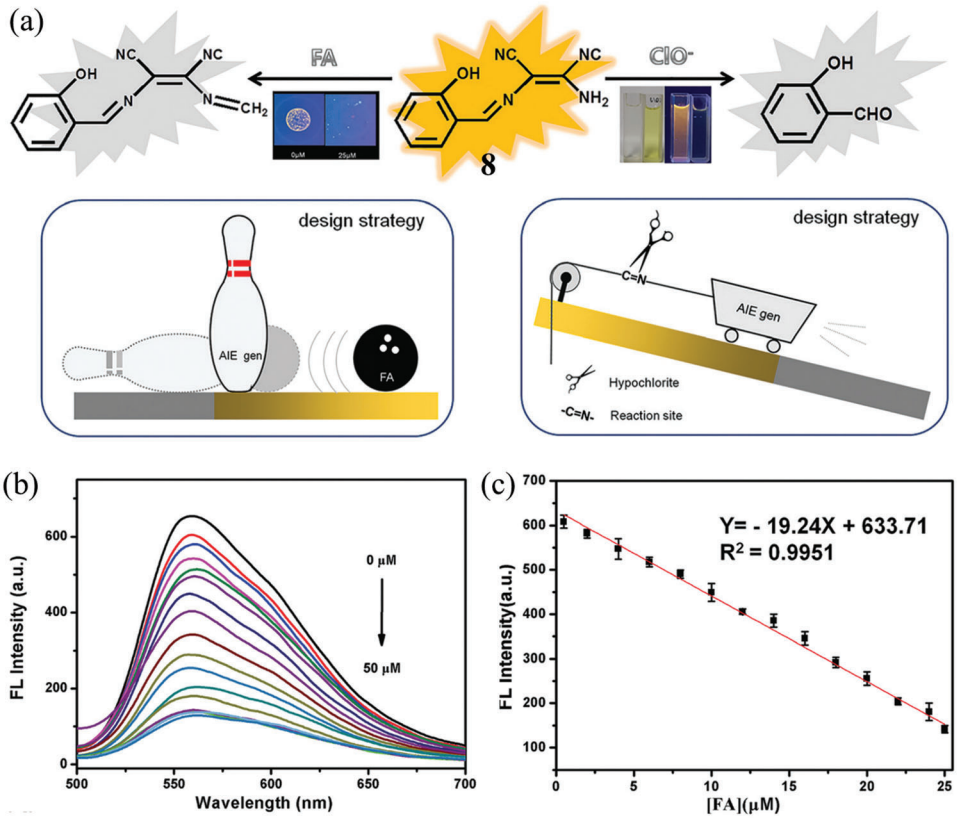

Figure 9. a) Mechanism of probe **8** for monitoring formaldehyde gas and hypochlorites. b) Fluorescence spectra and c) intensity of probe **8** at different concentrations of formaldehyde (0–25 mM). Reproduced with permission.[51] Copyright 2021, Royal Society of Chemistry.

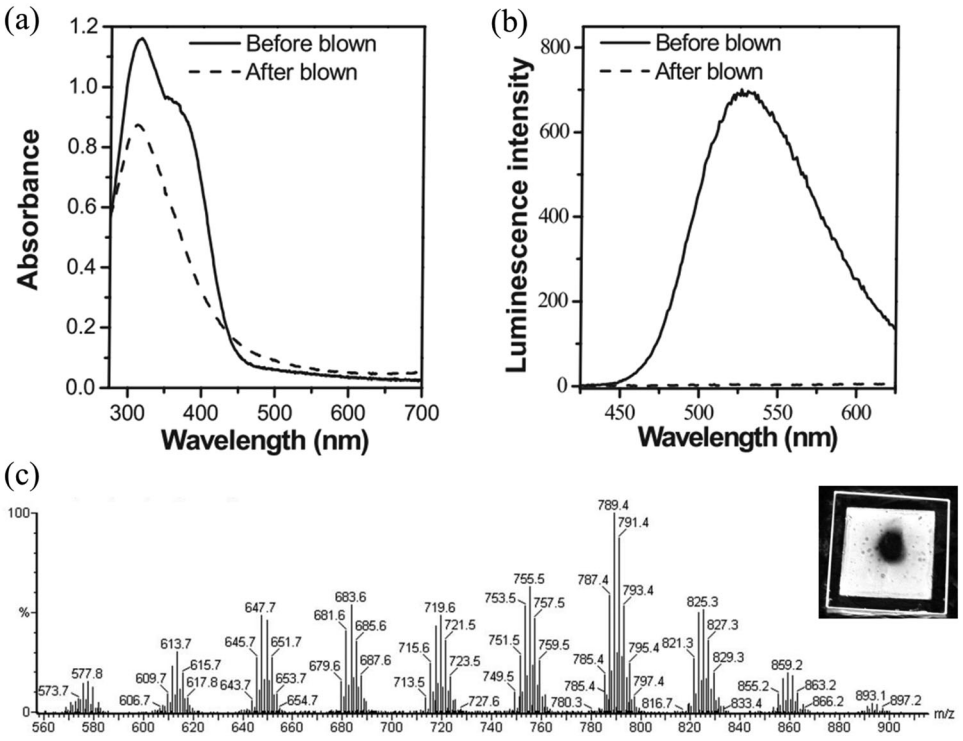

Figure 10. a) Absorbance and b) emission spectrum of probe **9** films before and after exposure to Cl_2. c) The mass spectrum of probe **9** after being treated with Cl_2. Reproduced with permission.[61] Copyright 2007, Wiley-VCH.

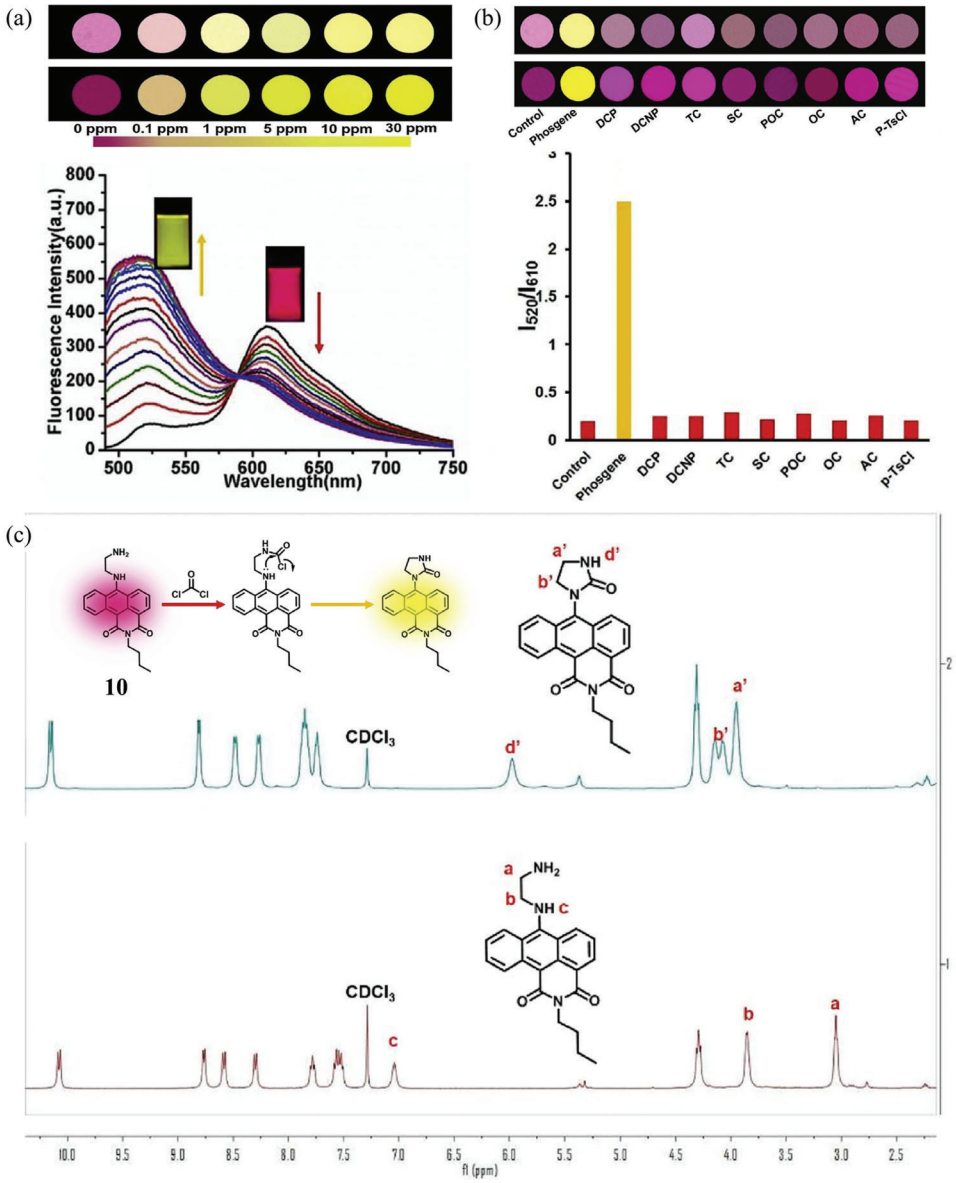

Figure 11. a) Photos of probe **10** on TLC plate without (top) and with (bottom) UV illumination exposure to different amounts of phosgene vapor for 1 min. The fluorescence emission spectrum of probe **10** with different concentrations of phosgene from 0 to 50 μM. b) Photos and fluorescence intensity ratio (I_{520}/I_{610}) of probe **10** on TLC plate without (top) and with (bottom) UV illumination exposure to phosgene (30 ppm), and various analytes (100 ppm): DCP (diethyl chlorophosphate), DCNP (diethyl cyanophosphonate), TC (thionylchloride, $SOCl_2$), SC (sulfuryl chloride, SO_2Cl_2), POC (phosphorus oxychloride, $POCl_3$), OC (oxalyl chloride, $(COCl)_2$), AC (acetyl chloride, CH_3COCl), p-TsCl (p-toluenesulfonyl chloride) for 1 min. c) ^{1}H NMR spectra of probe **10** before and after exposure to phosgene. Inset: the proposed mechanism of **10** for detecting phosgene. Reproduced with permission.[28] Copyright 2019, Elsevier.

3.6. Methanol and Ethanol

Alcohols are commonly used volatile organic compounds in industrial production and life, and the detection of their gaseous substances has always attracted much attention from academia and industry.[75] Among them, methanol, a commonly used industrial raw material, is toxic to the human body and can cause blindness, liver disease, and even death if consumed. Ethanol is relatively low in toxicity, but as the main ingredient in alcoholic beverages, it can easily enter the body, and excessive intake of ethanol can lead to social behaviors such as drunk driving.[76,77] Therefore, more convenient and efficient alcohol-based fluorescence sensors are needed.

Duan et al. designed an AIE fluorescent probe **13** with a donor–acceptor structure.[78] The fluorescence emission intensity of probe **13** was significantly enhanced when exposed to methanol or ethanol vapor. This is due to the formation of hydrogen bonds between probe **13** and alcohol molecules, which enhances the AIE effect and the intramolecular charge transfer. The higher the concentration of methanol or ethanol, the brighter probe **13** is.

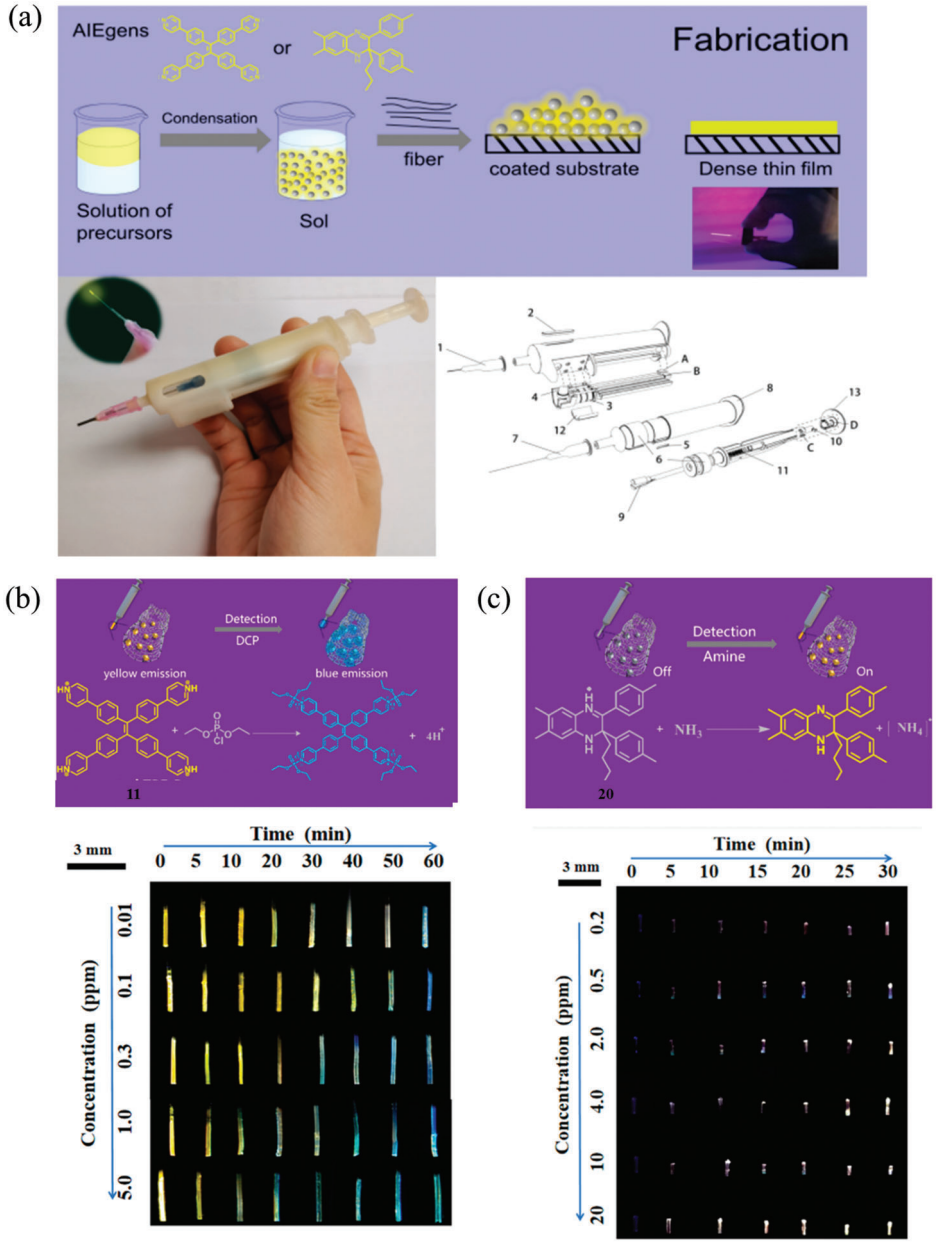

Figure 12. a) Scheme for fabrication and the structure of AIE handy pen. b) The mechanism of probe **11** detection DCP and the photos of probe **11**-coated fibers are exposed to different concentrations of DCP at different times under a UV lamp. c) Mechanism of probe **20** detection NH_3 and the photos of probe **20**-coated fibers exposure to different concentrations NH_3 at different times under UV illumination. Reproduced with permission.[27] Copyright 2021, ACS.

Based on this phenomenon, the limit of detection of methanol and ethanol was 8.02 ppm for the prepared portable thin film sensor (**Figure 14**).

3.7. Hydrazine (N_2H_4)

Hydrazine is a colorless and highly toxic compound commonly used in satellites, rocket fuel, boiler corrosion inhibitors, explosives, and antioxidants.[79] Hydrazine is strongly reducing and corrosive and can corrode glass, rubber, leather, cork, etc. Inhalation or contact with Hydrazine vapor can irritate the nose and upper respiratory tract, causing dizziness, nausea, vomiting, and central nervous system symptoms, which can cause eye damage.[80] Permanent damage, severe skin burns, neurasthenic syndrome, abnormal liver function, etc. may occur after long-term exposure.[81]

Liao et al. designed and synthesized a host–guest system to achieve N_2H_4 fluorescence sensing. AIE-active molecule **14** (labeled as TPM) can cooperate with cucurbit[8] uril (CB[8]), forming the complex of TMP@CB[8].[82] shows a deep red emission (625 nm), which is quickly turned into light yellow (525 nm) and

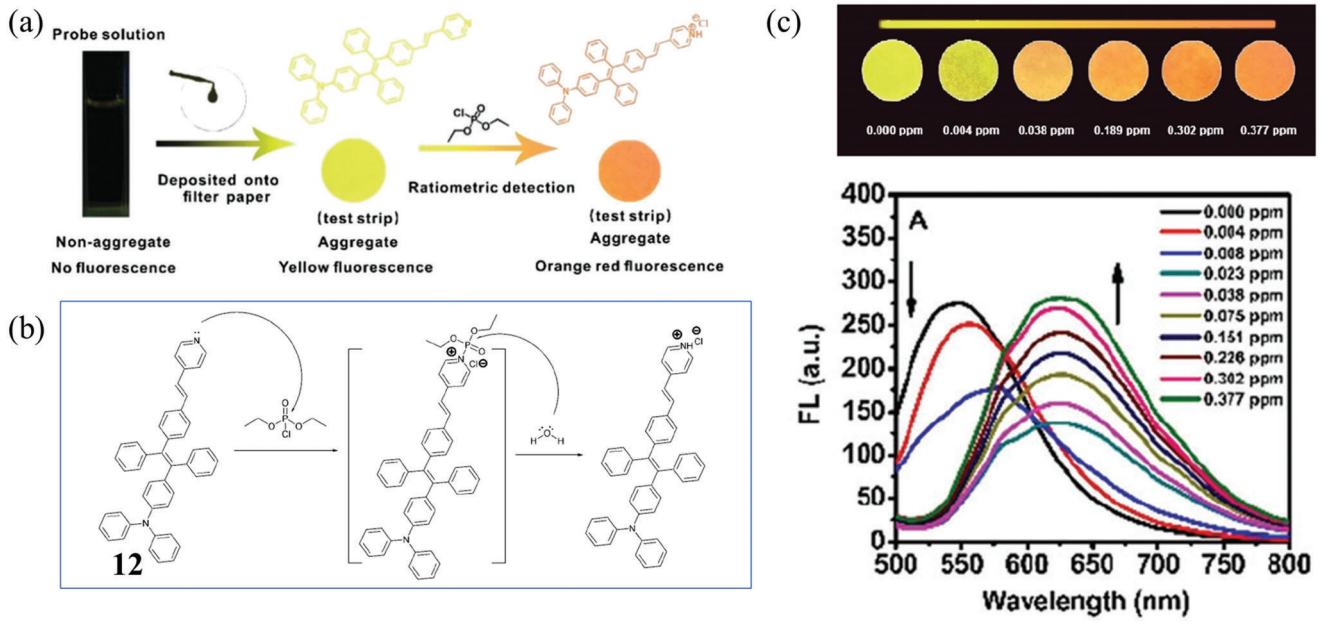

Figure 13. a) Preparation of probe **12** loaded test strips and the detection of DCP. b) Mechanism of probe **12** detection DCP. c) The photos and fluorescence spectrum of **12** under different DCP concentrations. All the photographs were taken under UV illumination. Reproduced with permission.[74] Copyright 2016, Royal Society of Chemistry.

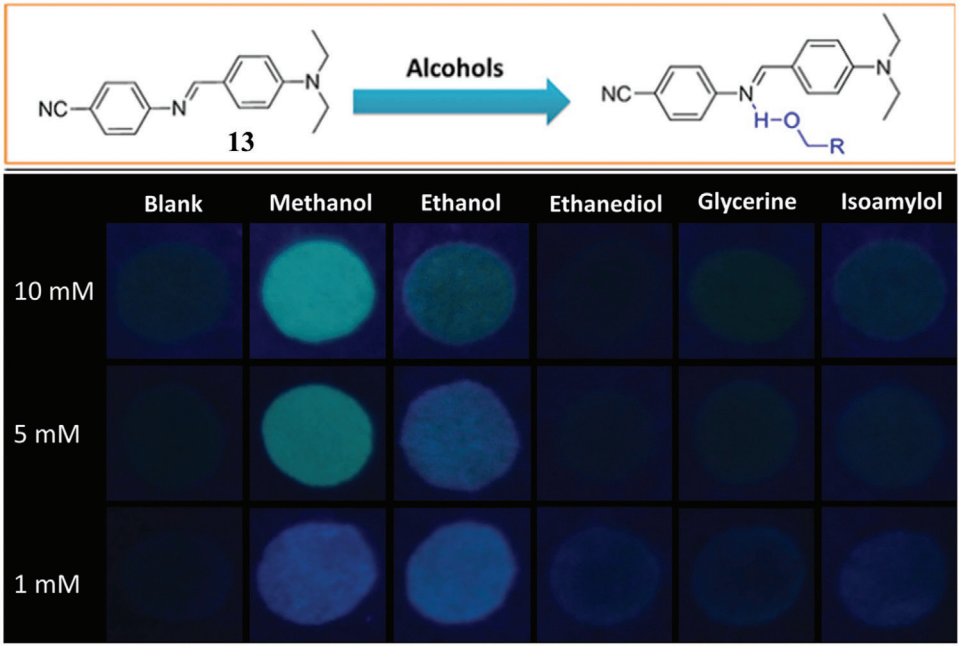

Figure 14. The proposed mechanism of probe **13** detects methanol and ethanol, and the photos of 13th sensor array taken under UV illumination show the great emission enhancement in response to different alcohols. Reproduced with permission.[78] Copyright 2021, Elsevier.

sky-blue (475 nm) as exposed to gaseous NH_3 and N_2H_4, respectively. The cyano group of fluorophore **14** is responsible for the N_2H_4 and NH_3 fluorescence sensing, as shown in **Figure 15**a. And TMP@CB[8] shows high sensitivity with a limit of detection for NH_3 and N_2H_4 of 0.80 and 0.41 ppm, respectively. In addition, TMP@CB[8] also exhibits an excellent selective sensing ability for NH_3 and N_2H_4 among the many analytes.

3.8. Acidic and Basic Gases

Acid- and base-responsive AIEgens exhibit both AIE effects and acidic/basic specific responses. Materials that can interact with acids and bases have groups that can accept or donate protons, such as phenolic hydroxyl groups (–OH), carboxyl groups (–COOH), amine groups (–NH_2), Schiff base structures (–CN–),

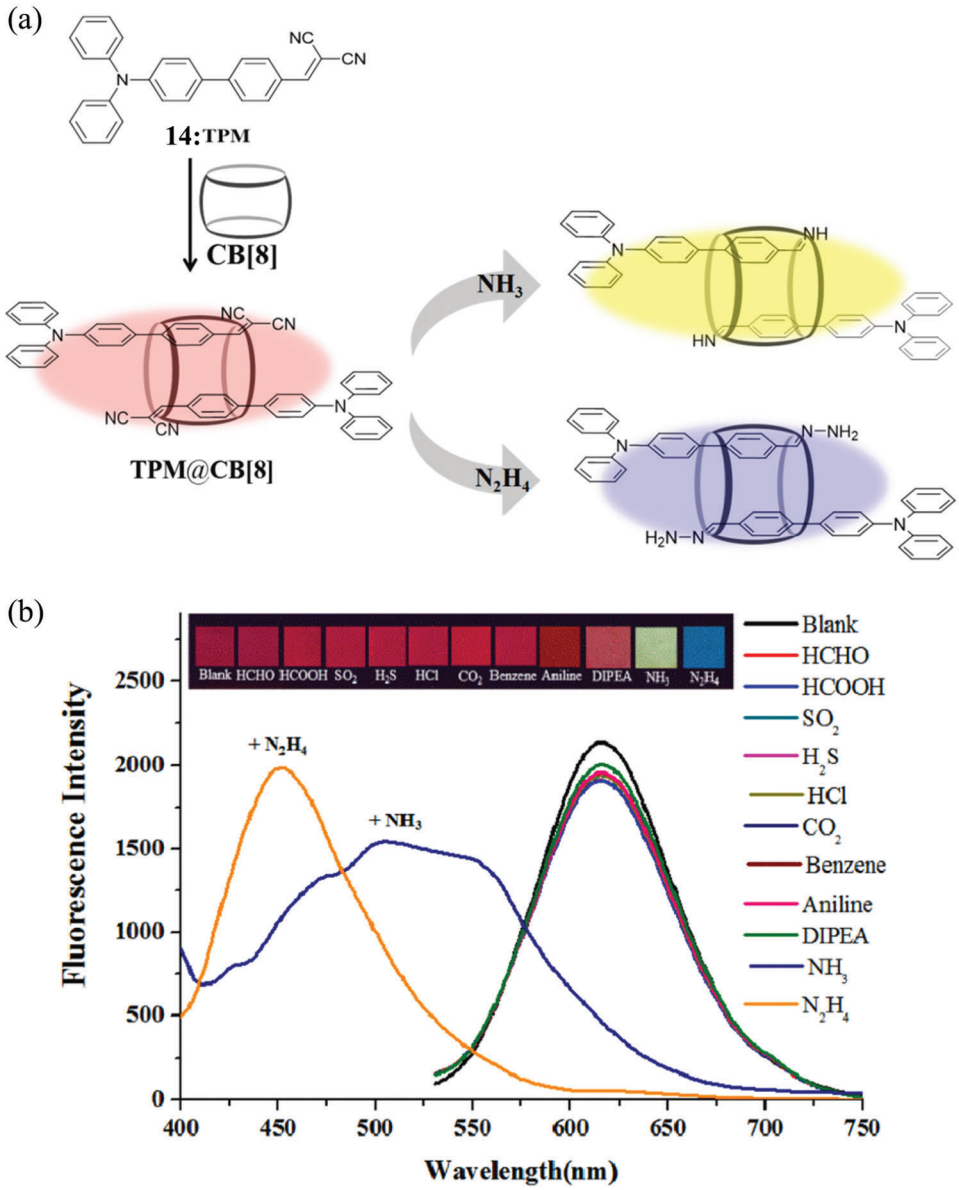

Figure 15. a) The schematic diagram of the fluorescence sensing of TMP@CB[8] (molecule **14**) toward gaseous NH_3 and N_2H_4. b) The fluorescence spectra of TMP@CB[8] without and with gaseous N_2H_4 (90 ppm), NH_3 (90 ppm), and other analytes (200 ppm). Insets: the photographs of test samples with different gaseous analytes under UV irradiation. Reproduced with permission.[82] opyright 2021, Elsevier.

and Pyridine group (–py), etc. Structurally, acidic/basic responsive AIE probes can be roughly divided into Schiff bases,[83] pyridinium salts,[84] indoles,[85] and thiazoles.[86]

Li et al.[29] cooperated AIE probe **15** with aminated mesoporous silica nanoparticles by a C=N bond and fabricated the complex into films by a dip-coating approach. The prepared film shows a blue-sky emission with a fluorescence peak at 485 nm, which decreases immediately with a red shift upon exposure to HCl gas as the protonation of nitrogen of the C=N bond unit. The film color change after exposure to HCl is visible directly by naked eyes. Surprisingly, the fluorescent recovery after exposure to NH_3 and the quenching and recovery can be repeated five cycles without too much change in the film (**Figure 16**b), suggesting this film could function as a two-channel gas sensor for both HCl and NH_3.

Gong et al. synthesized probes **16** and **17** for sensing gaseous HCl and NH_3. With benzothiazole enolate-ligand-based boron and asymmetrical propeller-shaped structures, probes **16** and **17** show AIE effect with a strong yellow emission at the solid state with a peak at 562 nm.[87] As the *N*, *N*-dimethylamino group in **16** and **17** can easily protonate by the acid. Their fluorescent color changes from yellow to orange after exposure to HCl and recovery after exposure to NH_3 (**Figure 17**b,d). The quenching and recovery can be repeated in several cycles without too much change in the film. Since **16** and **17** can realize reversible acid-base dual-channel fluorescence detection, it is a very promising and environmentally friendly probe.

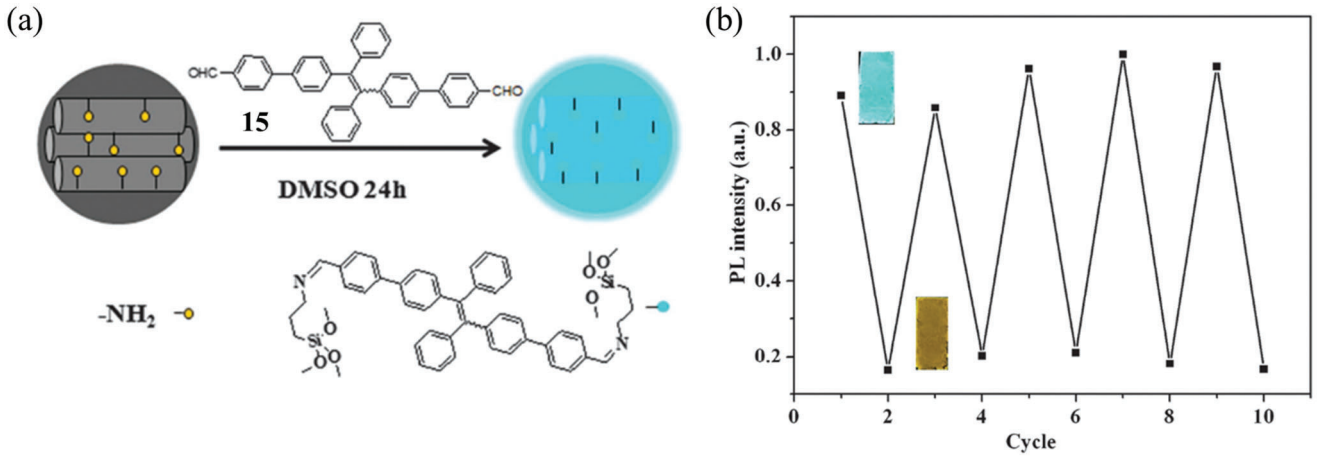

Figure 16. Synthetic route to cooperate AIE probe **15** with aminated mesoporous silica nanoparticles by a C=N bond. The fluorescent recovery cycles of as-made films. Points 2, 4, 6, 8, and 10 are the film after the exposure to HCl; Points 3, 5, 7, and 9 are the film exposed to NH_3. Reproduced with permission.[29] Copyright 2015, Royal Society of Chemistry.

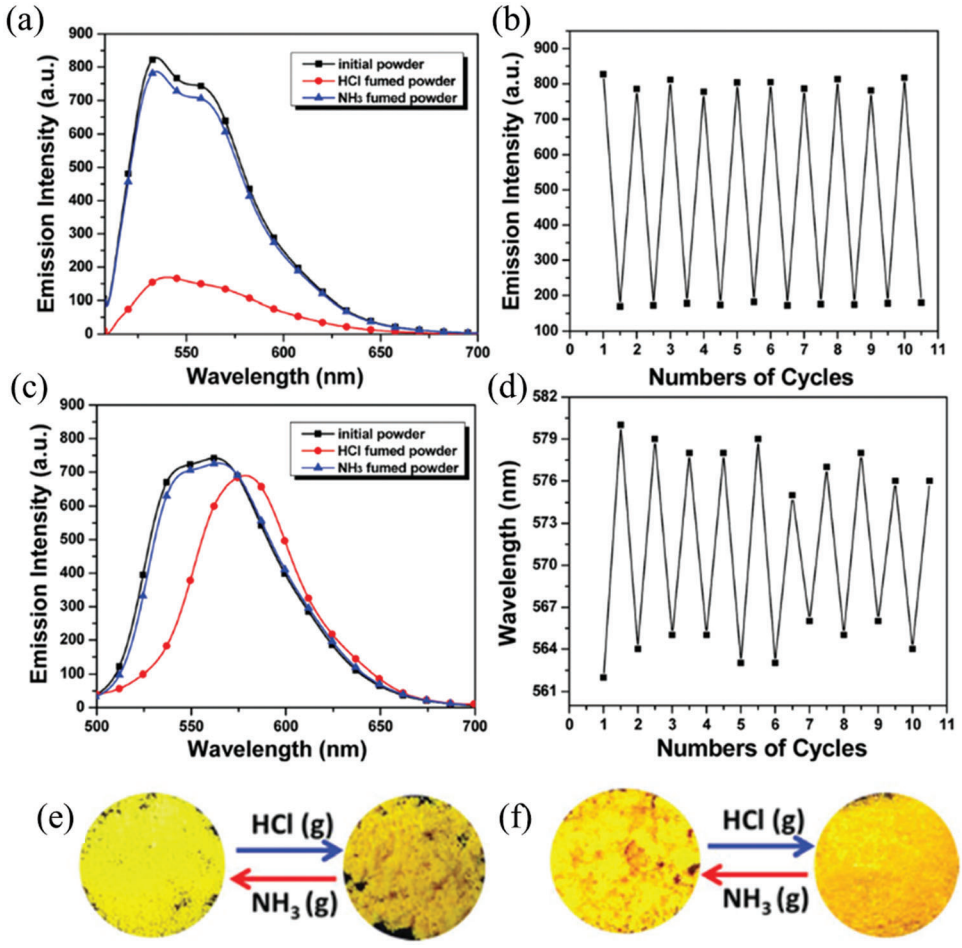

Figure 17. Fluorescence spectra of initial, HCl (g) and NH_3 (g) fumed powders of a) **16** and c) **17**; reversible switching of the emission of b) **16** and d) **17** by the HCl/NH_3 fuming cycle; Luminescence pictures of HCl and NH_3 fumed powders of e) **16** and f) **17**. Reproduced with permission.[87] Copyright 2015, Royal Society of Chemistry.

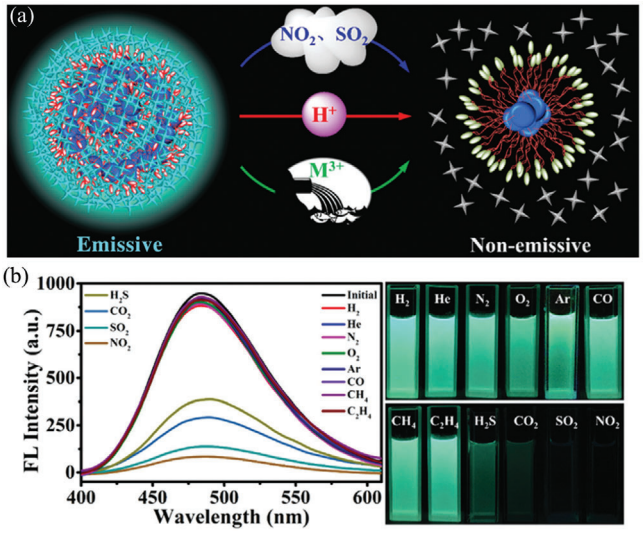

Figure 18. Proposed mechanism for detecting acid gases, protons, and M^{3+} based on probe **18** and **19** nanoparticles. Fluorescence spectra of **18** in THF/water mixtures respond to different gases. The concentration for all samples was 10^{-5} M. Reproduced with permission.[88] Copyright 2016, Royal Society of Chemistry.

Zuo et al. proposed a facile method to design fluorescent probes with the cooperation of AIE effects and dendritic polymers.[88] The rigid framework of polyhedral oligomeric silsesquioxane (POSS) units can firmly restrain the intramolecular motions of TPE in probes **18** and **19** and greatly improve the emission intensity in the aggregate state. After incorporating Schiff bases into POSS dendrimers and assembled into nanoparticles, it has pH response and acid gas detection capabilities, especially SO_2 and NO_2. It is well known that SO_2 and NO_2 are responsible for acid rain and environmental pollution. The primary pollutants seriously affect the natural environment and human health. When different gases were injected into the THF/water mixed solvent with probe **18**, it was found that the neutral gas did not affect the fluorescence of probe **18**. In contrast, the acid gas could quench its fluorescence in a short time (**Figure 18**b). This AIE probe and POSS synergistic product has a good and rapid identification ability for acid gas and is a promising fluorescent gas sensor material.

Flexible optical sensors are extensively studied and applied in many fields. However, developing sensitive and washable wearable sensors in optics for practical applications is still facing challenges.[89,90] Gao et al. prepared a flexible optical sensor based on AIE probes, which can realize reversible fluorescence detection of volatile acid-base gases.[91] The AIE probe **21** was assembled with periodic mesoporous silicone (PMO) framework by electrostatic spinning. The rigid framework of organosilica confines the movement of AIE molecules and enhances its fluorescence intensity in the solid state. At the same time, its three-dimensional ordered porous structure can ensure that the prepared gas sensor has a large specific surface area and is fully in contact with the gaseous reactants to achieve fast and sensitive detection performance (**Figure 19**). It is verified that the flexible sensor can reversibly detect acidic and basic gases, and its fluorescence intensity does not decrease significantly after multiple cycles. In addition, the as-prepared sensor exhibited good washability and good photostability (the fluorescence remained above 94% after 10 times of washing). This AIEgen silicone framework with diverse forms and ultra-stability for wearable and washable solid-state fluorescence shows great potential in smart gas sensors, wearable devices, and solid-state lighting applications.

3.9. Gas Pressure

Air pressure is one of the external forces that can change the form of molecular stacking/aggregation, affecting the fluorescence properties of AIEgens so that AIEgens can function as the gas pressure sensor. Lu et al. utilized AIE co-crystals to realize piezoelectric chromic materials with a wide response range and precise sensitivity.[92] Dicyandiphenyl derivatives are a new class of chromophores, widely used in sensors and optoelectronic devices, which can form co-crystals with different molecules. Adjusting the growth conditions, A and B/C (**22** in Scheme 1) can form a pressure-responsive co-crystal A-5B/A-2C. As shown in **Figure 20**, as the pressure gradually increases, the fluorescence intensity of the co-crystal A-2C gradually weakens, and the reversible enhancement of fluorescence is achieved after the pressure is restored (Figure 20b). This co-crystal structure-based AIE probe can respond to natural stress and display fluorescence or intrinsic color change, which can be used to detect the occurrence of damage.

Li et al. designed to probe **23** as a ligand to prepare an AIE-based metal-organic framework (MOF) that emits blue light in ambient conditions but barely emits light under vacuum conditions.[93] As the gas pressure increases, the emission intensity exhibits a smooth and reversible enhancement, and once the gas pressure is restored, the luminescent state recover. This phenomenon does not depend on the type of gas, and AIE-based MOF exhibits similar pressure-dependent fluorescence changes in the air, N_2, CO_2, and Ar, and exhibits excellent reversibility (**Figure 21**a–d). The X-ray diffraction patterns in standard atmospheric pressure and vacuum show that this may be due to the restriction of intramolecular motion due to structural deformation under pressure stimulation. As the pressure decreases, the **23** rotates counterclockwise by a certain angle, resulting in further adjacent suspended benzene rings. Separation, less restriction of intermolecular rotation, higher nonradiative decay rate, and ultimately lower fluorescence intensity. Here, the MOF structure provides a suitable matrix that enables the intramolecular motion of AIEgen to tune the luminescence response via gas pressure.

Table 1 summarizes all the above-mentioned AIE probes for gas sensors and their main properties to better understand the field.

4. Summary and Prospect

Benefiting from its high sensitivity and excellent selectivity, fluorescence sensing technology has been widely used in biochemical analysis, including qualitative and quantitative identification of gases. Organic small molecule materials are expected to be

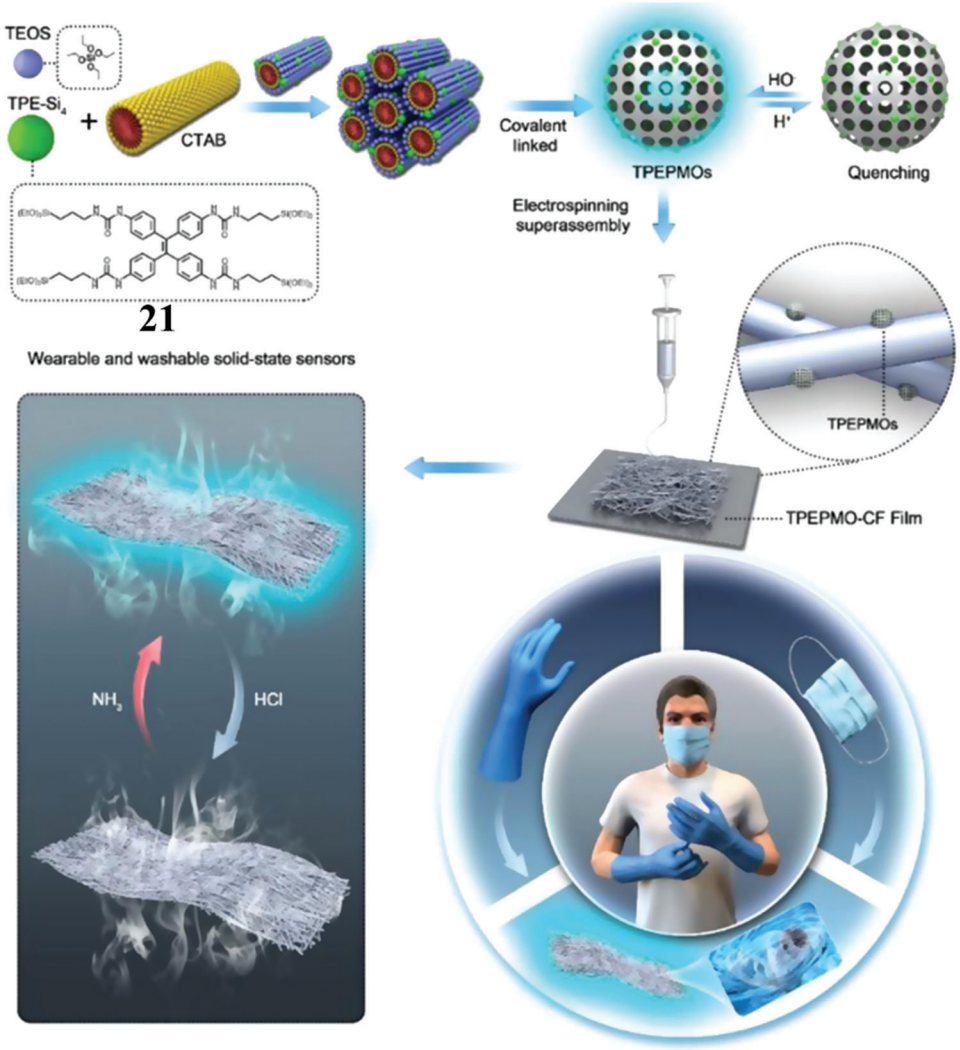

Figure 19. Illustration of the construction of probe **21** films for sensing applications. Reproduced with permission.[91] Copyright 2021, ACS.

commercial fluorescent sensor probes due to their low cost, environmental friendliness, precise and controllable structure, and easy functional modification. The traditional structurally planar ACQ-like molecules are unsuitable for application in solid-state probes due to their quenched fluorescence efficiency at high concentrations or in the aggregated state. AIEgens overcome the weakness of ACQ molecules and provide a new strategy for developing new fluorescent probes. Based on this, the review expounded the luminescence mechanism of AIEgens and its working mechanism as a gas fluorescent probe and enumerates the detection of different gases such as carbon dioxide, chlorine, nitrous oxide, acid gas, and air pressure by different AIEgens. It is convenient for readers to understand the research progress in this field and the design strategies for different gas probes.

Although AIE materials have made breakthroughs in the field of gas sensors, there are still some problems and challenges to be solved for practical applications. On one hand, the types and quantities of AIE probes currently developed are still limited, and the types of gases that can be detected and the detectable sensitivity need to be improved. There needs to be a more precise design strategy for different detection substances in order to obtain more AIE probes and screen products with commercial value; on one hand, the types and quantities of AIE probes currently developed are still limited, and the types of gases that can be detected and the detectable sensitivity need to be improved. It is necessary to have a more precise design strategy for different detection substances to obtain more AIE probes and screen products with commercial value. For acidic and alkaline gases, the detection mechanism of electrostatic interaction or hydrogen bond interaction, charge transfer or electron transfer is generally utilized, and corresponding response groups need to be added to the designed AIEgens. Considering the detection environment, it is more convenient for the AIEgens-based gas sensor to work in a thin film or other solid-state forms. And also, increasing the molecular luminescence property and enhancing the stokes shift of the aggregated state help to improve the sensitivity for detection. On the other hand, these studies are still in the research stage for the time being, only to prove the feasibility of

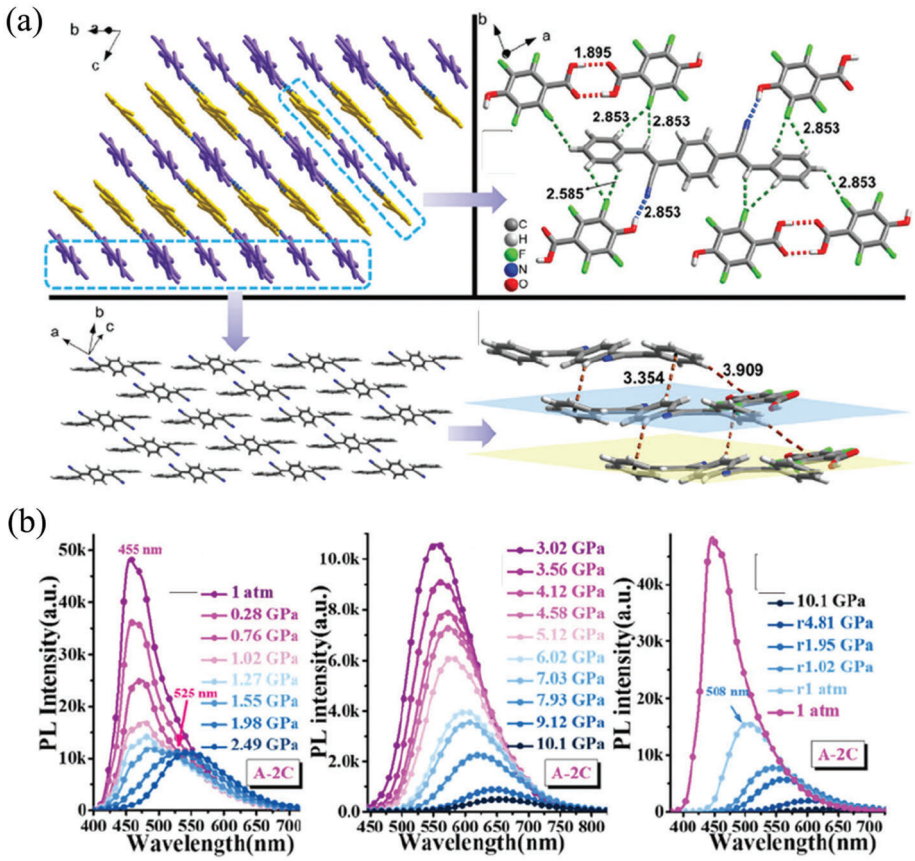

Figure 20. a) The molecular structures and stacking modes in co-crystal of A-2C (**22** in Scheme 1); b) In situ emission spectra of co-crystals A-2C under different pressure from1 atm to 10 GPa. Reproduced with permission.[92] Copyright 2018, Royal Society of Chemistry.

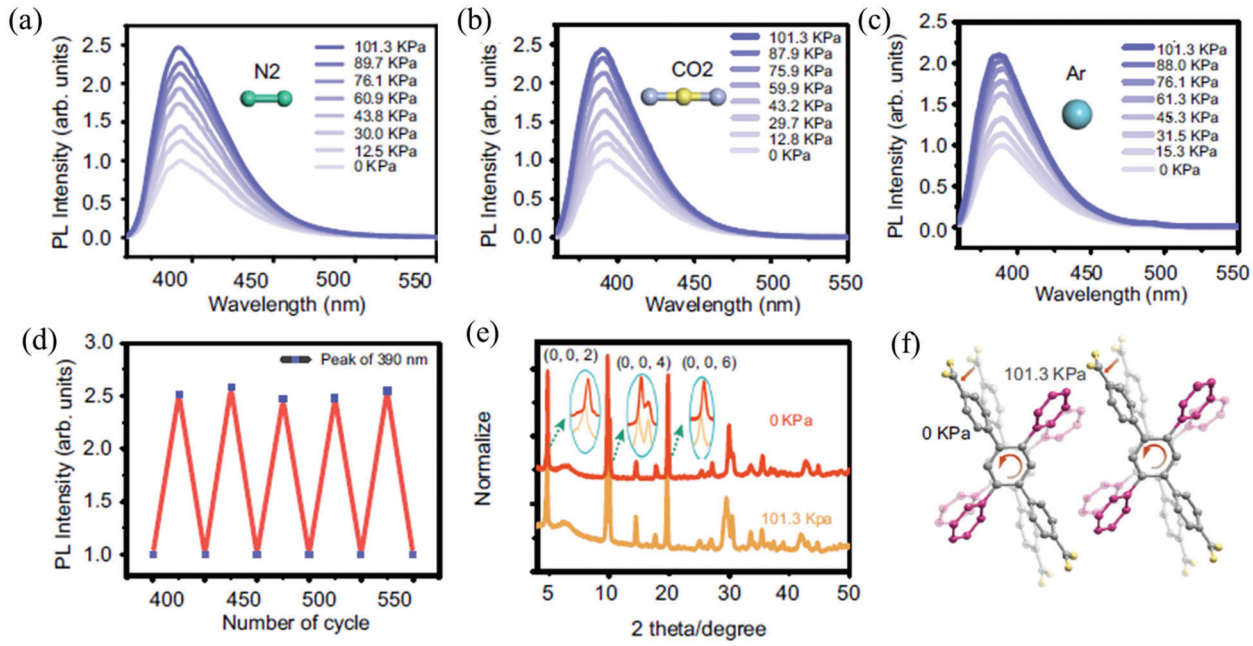

Figure 21. Gas–pressure-dependent fluorescence properties of MOF based on probe **23** in a) N_2, b) CO_2, and c) Ar. d) Reusability and stability luminescence response to the air pressure of multiple cycles. e) The X-ray diffraction patterns of at standard atmosphere and vacuum state and f) the proposed change of dangling phenyls. Reproduced with permission.[93] Copyright 2022, Springer Nature.

Table 1. Application of AIE probes in different gas.

Molecule	Emission peak [nm]	Target gas/vapor	Mechanism	Limit of detection (LOD)	Ref.
1	500	Chloroform and acetone	Non-reactive	NR	[39]
2	490	Chloroform and acetone	Non-reactive	NR	[39]
3	502	Chloroform and acetone	Non-reactive	NR	[39]
4	499	Chloroform and acetone	Non-reactive	NR	[39]
5	460	CO_2	Non-reactive	4.5 ppm	[43]
6	525	CO_2	Non-reactive	NR	[44]
7	525	Formaldehyde	Reactive	20 nM	[48]
8	525	Formaldehyde	Reactive	42 nM	[51]
9	542	Cl_2	Reactive	NR	[61]
10	520	Phosgene ($COCl_2$)	reactive	0.09 nM	[28]
11	425	Diethyl chlorophosphate and 1,2-dihydroquinoxaline	Reactive	3.4 ppb	[27]
12	546	Diethyl chlorophosphate	Reactive	1.82 ppb	[74]
13	504	Methanol and ethanol	Reactive	8.02 ppm	[78]
14	625	Ammonia and hydrazine	Reactive	0.80 and 0.41 ppm	[82]
15	485	HCl and NH_3	Non-reactive	NR	[29]
16	512	HCl and NH_3	Non-reactive	NR	[87]
17	510	HCl and NH_3	Non-reactive	NR	[87]
18	490	HCl, NO_2, SO_2	Non-reactive	NR	[88]
19	490	HCl, NO_2, SO_2	Non-reactive	NR	[88]
20	550	NH_3	Reactive	0.17 ppm	[27]
21	495	HCl and NH_3	Non-reactive	NR	[91]
22	455	Gas pressure and NH_3	Non-reactive	NR	[92]
23	390	Gas pressure	Non-reactive	NR	[93]

gas detection. There is still a long way to go until practical application. To sum up, with the unremitting persistence and efforts of scientists from multiple disciplines and fields, AIE probes in the area of gas probes and even the entire probe field will be rapidly developed, optimized, and upgraded. AIE materials with gas detection characteristics will be used in practice.

Acknowledgements

The authors thank the support of the National Natural Science Foundation of China (Grant No. 52027817) and Shenzhen Science and Technology Innovation Committee (Grant No. GJHZ20210705143204013) for funding support.

Conflict of Interest

The authors declare no conflict of interest.

Author Contributions

Y.Y. and S.Z. wrote the manuscript. J.J., F.M., J.Z., and C.H. participated in the discussion of the outline. T.H. and G.W. revised the manuscript. All authors discussed and commented on the manuscript.

Received: February 9, 2023
Revised: April 1, 2023
Published online: May 10, 2023

[1] O. S. Wolfbeis, *Anal. Chem.* **2006**, *78*, 3859.
[2] K. Cammann, *Phys. Chem. Chem. Phys.* **2003**, *5*, 5159.
[3] J. Watson, *Sens. Actuators* **1984**, *5*, 29.
[4] C. Hagleitner, A. Hierlemann, D. Lange, A. Kummer, N. Kerness, O. Brand, H. Baltes, *Nature* **2001**, *414*, 293.
[5] A. P. de Silva, D. B. Fox, T. S. Moody, S. M. Weir, *Trends Biotechnol.* **2001**, *19*, 29.
[6] R. Badugu, *J. Fluoresc.* **2005**, *15*, 71.
[7] F. Huang, J. Li, Z. Xu, Y. Liu, R. Luo, S. W. Zhang, P. Nie, Y. Lv, S. Zhao, W. Su, W. D. Li, S. Zhao, G. Wei, H. C. Kuo, F. Kang, *Nanomaterials* **2019**, *9*, 1312.
[8] H. N. Kim, M. H. Lee, H. J. Kim, J. S. Kim, J. Yoon, *Chem. Soc. Rev.* **2008**, *37*, 1465.
[9] H.-H. Wang, L. Xue, C.-L. Yu, Y.-Y. Qian, H. Jiang, *Dyes Pigm.* **2011**, *91*, 350.
[10] X. Y. Sun, T. Liu, J. Sun, X. J. Wang, *RSC Adv.* **2020**, *10*, 10826.
[11] D. Cao, Z. Liu, P. Verwilst, S. Koo, P. Jangjili, J. S. Kim, W. Lin, *Chem. Rev.* **2019**, *119*, 10403.
[12] J. B. Birks, *Photophysics of Aromatic Molecules*. Wiley, London **1970**.
[13] J. Luo, Z. Xie, J. W. Lam, L. Cheng, H. Chen, C. Qiu, H. S. Kwok, X. Zhan, Y. Liu, D. Zhu, B. Z. Tang, *Chem. Commun.* **2001**, *18*, 1740.
[14] J. Mei, Y. Hong, J. W. Lam, A. Qin, Y. Tang, B. Z. Tang, *Adv. Mater.* **2014**, *26*, 5429.
[15] J. Mei, N. L. Leung, R. T. Kwok, J. W. Lam, B. Z. Tang, *Chem. Rev.* **2015**, *115*, 11718.
[16] C. Xu, R. Ye, H. Shen, J. W. Y. Lam, Z. Zhao, B. Zhong Tang, *Angew. Chem., Int. Ed. Engl.* **2022**, *61*, e202204604.
[17] Y. Dong, J. W. Y. Lam, A. Qin, J. Liu, Z. Li, B. Z. Tang, J. Sun, H. S. Kwok, *Appl. Phys. Lett.* **2007**, *91*, 011111.

[18] Z. Zhao, X. Zheng, L. Du, Y. Xiong, W. He, X. Gao, C. Li, Y. Liu, B. Xu, J. Zhang, F. Song, Y. Yu, X. Zhao, Y. Cai, X. He, R. T. K. Kwok, J. W. Y. Lam, X. Huang, D. Lee Phillips, H. Wang, B. Z. Tang, *Nat. Commun.* **2019**, *10*, 2952.
[19] Y. Zhao, L. Zhang, Y. Liu, Z. Deng, R. Zhang, S. Zhang, W. He, Z. Qiu, Z. Zhao, B. Z. Tang, *Langmuir* **2022**, *38*, 8719.
[20] J. Zhang, P. Alam, S. Zhang, H. Shen, L. Hu, H. H. Y. Sung, I. D. Williams, J. Sun, J. W. Y. Lam, H. Zhang, B. Z. Tang, *Nat. Commun.* **2022**, *13*, 3492.
[21] X. He, H. Xie, L. Hu, P. Liu, C. Xu, W. He, W. Du, S. Zhang, H. Xing, X. Liu, H. Park, T. S. Cheung, M. H. Li, R. T. K. Kwok, J. W. Y. Lam, J. Lu, B. Z. Tang, *Aggregate* **2023**, *4*, e239.
[22] Z.-L. Gong, X. Zhu, Z. Zhou, S.-W. Zhang, D. Yang, B. Zhao, Y.-P. Zhang, J. Deng, Y. Cheng, Y.-X. Zheng, S.-Q. Zang, H. Kuang, P. Duan, M. Yuan, C.-F. Chen, Y. S. Zhao, Y.-W. Zhong, B. Z. Tang, M. Liu, *Sci. China: Chem.* **2021**, *64*, 2060.
[23] X. Huang, Q. Guo, R. Zhang, Z. Zhao, Y. Leng, J. W. Y. Lam, Y. Xiong, B. Z. Tang, *Compr. Rev. Food Sci. Food Saf.* **2020**, *19*, 2297.
[24] M. Shimizu, T. Sakurai, *Aggregate* **2022**, *3*, e144.
[25] Q. Peng, Z. Shuai, *Aggregate* **2021**, *2*, e91.
[26] R. Ma, J. Yu, T. Liu, G. Zhang, Y. Xiao, Z. Luo, G. Chai, Y. Chen, Q. Fan, W. Su, G. Li, E. Wang, X. Lu, F. Gao, B. Tang, H. Yan, *Aggregate* **2022**, *3*, e58.
[27] X. Huang, Z. Jiao, Z. Guo, J. Yang, P. Alam, Y. Liu, Y. Men, P. Zhang, H. Feng, S. Yao, B. Z. Tang, *ACS Mater. Lett.* **2021**, *3*, 249.
[28] P. Liu, N. Liu, C. Liu, Y. Jia, L. Huang, G. Zhou, C. Li, S. Wang, *Dyes Pigm.* **2019**, *163*, 489.
[29] D. Li, Y. Zhang, Z. Fan, J. Yu, *Chem. Commun.* **2015**, *51*, 13830.
[30] N. Yamazoe, *Sens. Actuators, B* **2005**, *108*, 2.
[31] H. Nazemi, A. Joseph, J. Park, A. Emadi, *Sensors* **2019**, *19*, 1285.
[32] N. Yamazoe, K. Shimanoe, *Sens. Actuators, B* **2009**, *138*, 100.
[33] M. C. DeRosa, D. J. Hodgson, G. D. Enright, B. Dawson, C. E. Evans, R. J. Crutchley, *J. Am. Chem. Soc.* **2004**, *126*, 7619.
[34] J.-S. Yang, T. M. Swager, *J. Am. Chem. Soc.* **1998**, *120*, 11864.
[35] B. Li, Z. He, H. Zhou, H. Zhang, T. Cheng, *Chin. Chem. Lett.* **2017**, *28*, 1929.
[36] Z. Zhou, X. Li, Y. Zhang, C. C. Zhang, Y. Tang, J. Gao, L. Ma, Q. Wang, *Mater. Sci. Eng., C* **2019**, *99*, 1092.
[37] H. Ren, F. Huo, Y. Zhang, S. Zhao, C. Yin, *Sens. Actuators, B: Chem.* **2020**, *319*, 128248.
[38] W. Shen, J. Yu, J. Ge, R. Zhang, F. Cheng, X. Li, Y. Fan, S. Yu, B. Liu, Q. Zhu, *ACS Appl. Mater. Interfaces* **2016**, *8*, 927.
[39] Y. Dong, J. W. Y. Lam, A. Qin, Z. Li, J. Sun, Y. Dong, B. Z. Tang, *J. Inorg. Organomet. Polym. Mater.* **2007**, *17*, 673.
[40] L. de Lary, A. Loschetter, O. Bouc, J. Rohmer, C. M. Oldenburg, *Int. J. Greenhouse Gas Control* **2012**, *9*, 322.
[41] R. S. Haszeldine, *Science* **2009**, *325*, 1647.
[42] C.-S. Chu, Y.-L. Lo, *Sens. Actuators, B* **2008**, *129*, 120.
[43] Y. Ma, M. Cametti, Z. Džolić, S. Jiang, *J. Mater. Chem. C* **2018**, *6*, 9232.
[44] M. H. Xie, W. Cai, X. Chen, R. F. Guan, L. M. Wang, G. H. Hou, X. G. Xi, Q. F. Zhang, X. L. Yang, R. Shao, *ACS Appl. Mater. Interfaces* **2018**, *10*, 2868.
[45] O. Merk, G. Speit, *Environ. Mol. Mutagen.* **1998**, *32*, 260.
[46] R. G. Liteplo, M. E. Meek, *J. Toxicol. Environ. Health, Part B* **2003**, *6*, 85.
[47] X. Tang, Y. Bai, A. Duong, M. T. Smith, L. Li, L. Zhang, *Environ. Int.* **2009**, *35*, 1210.
[48] A. Bi, T. Gao, X. Cao, J. Dong, M. Liu, N. Ding, W. Liao, W. Zeng, *Sens. Actuators, B* **2018**, *255*, 3292.
[49] C. Liu, C. Shi, H. Li, W. Du, Z. Li, L. Wei, M. Yu, *Sens. Actuators, B* **2015**, *219*, 185.
[50] Q. Lin, Y.-Q. Fan, G.-F. Gong, P.-P. Mao, J. Wang, X.-W. Guan, J. Liu, Y.-M. Zhang, H. Yao, T.-B. Wei, *ACS Sustainable Chem. Eng.* **2018**, *6*, 8775.
[51] X. Wen, L. Yan, Z. Fan, *New J. Chem.* **2021**, *45*, 8155.
[52] X. Wen, Z. Fan, *Anal. Chim. Acta* **2016**, *945*, 75.
[53] L. Yan, X. Wen, Z. Fan, *Anal. Bioanal. Chem.* **2020**, *412*, 1453.
[54] X. Wen, Z. Fan, *Sens. Actuators, B* **2017**, *247*, 655.
[55] A. K. Sharma, A. Mahajan, R. Saini, R. K. Bedi, S. Kumar, A. K. Debnath, D. K. Aswal, *Sens. Actuators, B* **2018**, *255*, 87.
[56] T. Fu, *Sens. Actuators, B* **2007**, *123*, 1113.
[57] K. Brudzewski, *Sens. Actuators, B* **1992**, *9*, 59.
[58] S. Kumar, N. Kaur, A. K. Sharma, A. Mahajan, R. K. Bedi, *RSC Adv.* **2017**, *7*, 25229.
[59] R. H. Bari, S. B. Patil, *Sens. Lett.* **2015**, *13*, 185.
[60] X. Zhao, Z. Li, X. Lou, M. Li, N. Zhang, *J. Adv. Ceram.* **2013**, *2*, 31.
[61] Z. Ning, Z. Chen, Q. Zhang, Y. Yan, S. Qian, Y. Cao, H. Tian, *Adv. Funct. Mater.* **2007**, *17*, 3799.
[62] A. T. Balaban, P. T. Frangopol, M. Frangopol, N. Negoiţă, *Tetrahedron* **1967**, *23*, 4661.
[63] T. Naddo, Y. Che, W. Zhang, K. Balakrishnan, X. Yang, M. Yen, J. Zhao, J. S. Moore, L. Zang, *J. Am. Chem. Soc.* **2007**, *129*, 6978.
[64] C. B. Bast, D. F. Glass, *Handbook of Toxicology of Chemical Warfare Agents*, Elsevier, Boston **2015**.
[65] C. Li, H. Ji, Y. Cai, D. A. Ayana, P. Lv, M. Liu, Y. Jiang, *J. Interferon Cytokine Res.* **2013**, *33*, 612.
[66] Y. Hu, L. Chen, H. Jung, Y. Zeng, S. Lee, K. M. Swamy, X. Zhou, M. H. Kim, J. Yoon, *ACS Appl. Mater. Interfaces* **2016**, *8*, 22246.
[67] N. C. Staub, *Physiol. Rev.* **1974**, *54*, 678.
[68] A. M. Sciuto, P. T. Strickland, T. P. Kennedy, Y. L. Guo, G. H. Gurtner, *J. Appl. Physiol.* **1996**, *80*, 149.
[69] V. V. Singh, K. Kaufmann, B. Esteban-Fernandez de Avila, M. Uygun, J. Wang, *Chem. Commun.* **2016**, *52*, 3360.
[70] M. R. Sambrook, S. Notman, *Chem. Soc. Rev.* **2013**, *42*, 9251.
[71] J. Yao, Y. Fu, W. Xu, T. Fan, Y. Gao, Q. He, D. Zhu, H. Cao, J. Cheng, *Anal. Chem.* **2016**, *88*, 2497.
[72] H. J. Kim, J. H. Lee, H. Lee, J. H. Lee, J. H. Lee, J. H. Jung, J. S. Kim, A Mesoporous, *Adv. Funct. Mater.* **2011**, *21*, 4035.
[73] J. G. Weis, T. M. Swager, *ACS Macro Lett.* **2015**, *4*, 138.
[74] S. Huang, Y. Wu, F. Zeng, L. Sun, S. Wu, *J. Mater. Chem. C* **2016**, *4*, 10105.
[75] R. Kavet, K. M. Nauss, *Crit. Rev. Toxicol.* **1990**, *21*, 21.
[76] H. Y. Li, S. N. Zhao, S. Q. Zang, J. Li, *Chem. Soc. Rev.* **2020**, *49*, 6364.
[77] P. D. Thungon, A. Kakoti, L. Ngashangva, P. Goswami, *Biosens. Bioelectron.* **2017**, *97*, 83.
[78] Y. Duan, Y. Liu, H. Han, X. Zhang, M. Zhang, Y. Liao, T. Han, *Spectrochim. Acta, Part A* **2021**, *252*, 119515.
[79] S. K. Manna, A. Gangopadhyay, K. Maiti, S. Mondal, A. K. Mahapatra, *ChemistrySelect* **2019**, *4*, 7219.
[80] S. Garrod, M. E. Bollard, A. W. Nicholls, S. C. Connor, J. Connelly, J. K. Nicholson, E. Holmes, *Chem. Res. Toxicol.* **2005**, *18*, 115.
[81] C. Batchelor-McAuley, C. E. Banks, A. O. Simm, T. G. Jones, R. G. Compton, *Analyst* **2006**, *131*, 106.
[82] S. Liao, J. Fang, Y. Li, X. Chen, C. Gao, D. Tian, W. Li, *Sens. Actuators, B: Chem.* **2021**, *349*, 130749.
[83] P. Song, X. Chen, Y. Xiang, L. Huang, Z. Zhou, R. Wei, A. Tong, *J. Mater. Chem.* **2011**, *21*, 13470.
[84] J. Zhang, J. Chen, B. Xu, L. Wang, S. Ma, Y. Dong, B. Li, L. Ye, W. Tian, *Chem. Commun.* **2013**, *49*, 3878.
[85] S. Chen, Y. Hong, Y. Liu, J. Liu, C. W. Leung, M. Li, R. T. Kwok, E. Zhao, J. W. Lam, Y. Yu, B. Z. Tang, *J. Am. Chem. Soc.* **2013**, *135*, 4926.
[86] C. Ma, B. Xu, G. Xie, J. He, X. Zhou, B. Peng, L. Jiang, B. Xu, W. Tian, Z. Chi, S. Liu, Y. Zhang, J. Xu, *Chem. Commun.* **2014**, *50*, 7374.
[87] S. Gong, Q. Liu, X. Wang, B. Xia, Z. Liu, W. He, *Dalton Trans.* **2015**, *44*, 14063.

[88] Y. Zuo, X. Wang, Y. Yang, D. Huang, F. Yang, H. Shen, D. Wu, *Polym. Chem.* **2016**, *7*, 6432.
[89] R. Tao, Y. Zhao, H. Chu, A. Wang, J. Zhu, X. Chen, Y. Zou, M. Shi, R. Liu, N. Su, J. Du, H. M. Zhou, L. Zhu, X. Qian, H. Liu, J. Loscalzo, Y. Yang, *Nat. Methods* **2017**, *14*, 720.
[90] S. Yao, P. Ren, R. Song, Y. Liu, Q. Huang, J. Dong, B. T. O'Connor, Y. Zhu, *Adv. Mater.* **2020**, *32*, e1902343.
[91] M. Gao, G. Xu, R. Zhang, Z. Liu, H. Xia, B. Shao, C. Xue, J. Li, S. Miao, W. Fu, X. Zhang, J. Zhou, X. Jiang, K. Liang, B. Kong, *Anal. Chem.* **2021**, *93*, 2367.
[92] B. Lu, Y. Zhang, X. Yang, K. Wang, B. Zou, D. Yan, *J. Mater. Chem. C* **2018**, *6*, 9660.
[93] Z. Li, F. Jiang, M. Yu, S. Li, L. Chen, M. Hong, *Nat. Commun.* **2022**, *13*, 2142.

Yongbo Yu received his master's and bachelor's degrees from Xuzhou Medical University, majoring in medicinal chemistry. He is about to start his doctoral study at Central China Normal University. His main research interests are organic synthesis, drug development and design, and multifunctional fluorescent probes.

Zhang Siwei received her bachelor's degree from the Beijing University of Science and Technology and her doctorate from Tsinghua University. She is currently conducting postdoctoral research in the Department of Chemistry, at the Hong Kong University of Science and Technology. Dr. Zhang's research interests are the mechanism of aggregation-induced emission and the application of aggregation-induced luminescence molecules in optoelectronics and biology.

Guodan Wei is an associate professor and principal investigator (PI) at Tsinghua Shenzhen International Graduate School, Tsinghua University, China. Her main research area has been focusing on innovative optoelectronics materials and their applications for OLEDs, solar cells and photodetectors for wearable and flexible bright future. Up to new, she has published more than 140 papers and cited for > 3750 with h-index of 29.